Pergamon

Geochimica et Cosmochimica Acta, Vol. 62, No. 14, pp. 2535–2553, 1998

0016-7037/98 $19.00 + .00

PII S0016-7037(98)00166-5

A petrologic and isotopic study of winonaites: Evidence for early partial melting, brecciation, and metamorphism

G. K. Benedix,[1,*] T. J. McCoy,[2] K. Keil,[1,†] D. D. Bogard,[3] and D. H. Garrison[3]

[1]Hawaii Institute of Geophysics and Planetology, School of Ocean and Earth Science and Technology, University of Hawaii at Manoa, Honolulu, Hawaii 96822, USA
[2]Dept. of Mineral Sciences, MRC NHB-119, National Museum of Natural History, Smithsonian Institution, Washington, D.C., 20560, USA
[3]Code SN2, NASA/Johnson Space Center, Houston, Texas 77058, USA

(*Received April* 22, 1997; *accepted in revised form April* 16, 1998)

Abstract—We have conducted detailed petrologic, chemical, and isotopic studies of winonaites to ascertain the genesis of this group of meteorites. Winonaites have reduced mineral compositions and mineralogy, and oxygen isotopic compositions distinct from primitive achondrite groups other than silicate inclusions in IAB and IIICD irons. However, winonaites differ from IAB and IIICD irons in that they lack the metallic matrices of the latter and consist mostly of silicates. On the basis of these criteria, Winona, Mount Morris (Wisconsin), Tierra Blanca, Pontlyfni, Y-74025, Y-75300, Y-8005, and QUE 94535 are winonaites and Y-75305 and Y-75261 may be winonaites. Winonaites are fine- to medium-grained, mostly equigranular rocks. Pontlyfni and Mount Morris (Wisconsin) contain what appear to be relict chondrules. Several winonaites contain mm-sized areas that differ substantially in grain size and/or silicate mineralogy from the surrounding matrix. Fe,Ni-FeS veins are common in many winonaites. Mineral compositions are intermediate between E and H chondrites, and reduced sulfides are observed in low-FeO winonaites. Bulk major element compositions are roughly chondritic, although REE elements are fractionated. The ^{39}Ar-^{40}Ar ages of three winonaites range from $\geq$4.40 Ga (Mount Morris, Wisconsin) to 4.54 Ga (Pontlyfni). Cosmic-ray exposure ages are $\sim$20–80 Ma. Trapped noble gases in these winonaites resemble those in enstatite chondrites. We suggest that the winonaites formed from a chondritic precursor material unlike that of known chondrites in mineral and oxygen isotopic compositions, and this material may have been heterogeneous in composition. Extensive heating caused metamorphism and partial melting of both Fe,Ni-FeS and silicate material. Impact brecciation during cooling mixed lithologies with different thermal histories, and subsequent metamorphism produced recrystallization, grain growth, and reduction of mafic silicates. The ^{39}Ar-^{40}Ar ages indicate that cooling may have been more rapid than observed in IAB irons, although later resetting may have occurred. *Copyright © 1998 Elsevier Science Ltd*

1. INTRODUCTION

Detailed studies of asteroidal meteorites suggest that some asteroids are primitive and never melted, whereas others melted and differentiated into cores, mantles, and crusts (e.g., 4 Vesta; Gaffey et al., 1993). However, some meteorites exhibit features intermediate between primitive chondrites and the more evolved achondrites and irons. These rocks experienced incomplete partial melting, and their properties offer insights into and constraints on the geologic processes which occurred on small bodies in the early solar system. Several groups of meteorites which experienced incomplete partial melting have been recognized, and these are collectively labeled "primitive achondrites" (Prinz et al., 1983). These rocks are characterized by chondritic bulk elemental compositions and chondritic mineral assemblages and by textures that vary from metamorphic to those suggesting partial melting. These groups include the acapulcoites and lodranites (Nagahara, 1992; Takeda et al., 1994; Mittlefehldt et al., 1996; McCoy et al., 1996b, 1997a, b), silicate inclusions in IAB irons (e.g., Bunch et al., 1970; Bild, 1977; Choi et al., 1995) and IIICD irons (McCoy et al., 1993), brachinites (Nehru et al., 1996; Swindle et al., 1998), and winonaites (e.g., Graham et al., 1977; Prinz et al., 1980; Kimura et al., 1992).

In this paper, we concentrate on the petrologic, chemical, and isotopic features of the winonaites. Previous investigators have studied only individual winonaites (e.g., Tierra Blanca; King et al., 1981) or a subset of the winonaites (e.g., Graham et al., 1977; Kimura et al., 1992). In contrast, we examined all members of the winonaite group. This is also the first study that concentrates on the textural features, whereas previous authors have focused primarily on mineral and bulk elemental compositions. It should be noted that silicate inclusions in IAB irons resemble the winonaites compositionally, mineralogically, and texturally. We discuss these meteorites and the relationship between winonaites and IAB irons in another paper (Benedix et al., 1998).

Here, we discuss the criteria for classification of winonaites and list the members of this group. We discuss the properties of the group, with special emphasis on textural features and ^{39}Ar-^{40}Ar ages. We also discuss implications for the nature of the precursor chondritic material and the heating, partial melting, metamorphism, and brecciation experienced by these rocks.

2. CLASSIFICATION

Three criteria are used to classify the winonaites: (1) The highly reduced mineralogy and mineral compositions, (2) the

*Present address: NASA/Ames Research Center, MS 245-3, Moffett Field, California 94035-1000, USA (gbenedix@mail.arc.nasa.gov).
†Also associated with the Hawaii Center for Volcanology.

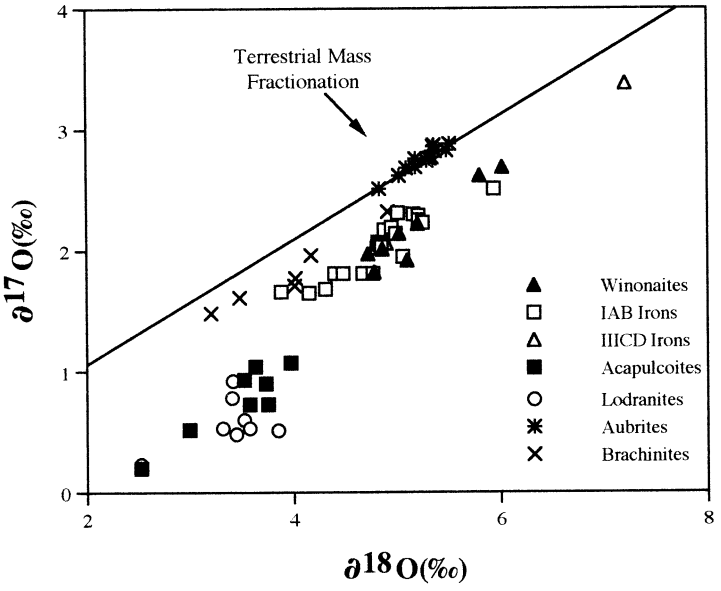

Fig. 1. Oxygen isotopic compositions for a variety of primitive achondrites (Clayton and Mayeda, 1996). Winonaites can be clearly distinguished from acapulcoites, lodranites, brachinites, and aubrites, but overlap with silicate inclusions in IAB and IIICD irons. Shown are the winonaites Winona, Mount Morris (Wisconsin), Pontlyfni, Tierra Blanca, QUE 94535, Y-74025, Y-75300, and Y-75261.

oxygen isotopic compositions, and (3) the abundance and distribution of metal and troilite. Previous workers (e.g., Mason and Jarosewich, 1967; Graham et al., 1977; Prinz et al., 1980; Bild, 1977; Kimura et al., 1992) have demonstrated that the olivines of the winonaites are Mg-rich ($Fa_{<5}$). In addition, the winonaites contain some characteristic accessory minerals including alabandite, daubreélite, schreibersite, and chromite. Most of the winonaites are fine-grained and have granulitic textures. However, these criteria alone cannot distinguish winonaites from all other primitive achondrites such as the acapulcoites, some of which are also highly reduced (e.g., ALH A81187/84190, $Fa_{4.2}$) and have fine-grained, granulitic textures (McCoy et al., 1996).

A more useful criterion of classification is the oxygen isotopic composition (Clayton and Mayeda, 1996). These data establish the winonaites as a group and allow discrimination from acapulcoites and lodranites as well as some other groups of meteorites (e.g., ureilites, brachinites). The oxygen isotopic compositions of the winonaites are identical to those of silicate inclusions in IAB and IIICD irons (Fig. 1).

Members of the winonaite group which satisfy both the oxygen isotopic composition and mineralogical criteria include Winona, Pontlyfni, Tierra Blanca, Mount Morris (Wisconsin), Yamato 74025, Yamato 75300, Yamato 75305, Yamato 8005, and QUE 94535 (Graham et al., 1977; Prinz et al., 1980; King et al., 1981; Kimura et al., 1992; Clayton and Mayeda, 1996; Mason, 1996; Yugami et al., 1996; R. N. Clayton, pers. commun., 1996). Yamato 75261 has tentatively been classified as a winonaite based on oxygen isotopic composition (Clayton and Mayeda, 1996). We have included literature data in addition to our own results on these meteorites where available.

3. SAMPLES AND TECHNIQUES

We have concentrated our study on those meteorites (Table 1) for which previously published mineralogical descriptions and oxygen isotopic compositions confirm classification as winonaites. Where pos-

TABLE 1. Winonaites studied and sources of material.

Meteorite	Section	Source
Winona	USNM 854-1	Smithsonian Institution
	UH 133	University of Hawaii
	UH 195	University of Hawaii
Mt. Morris (Wis.)	USNM 1198-1	Smithsonian Institution
	USNM 1198-2	Smithsonian Institution
	UH 157	University of Hawaii
Tierra Blanca	M-3, K1	Elbert King, Univ. of Houston
	M-3, K1	Elbert King, Univ. of Houston
Pontlyfni	BM1975, M6 P1242	British Museum
	BM1975, M6_2	British Museum
	BM1975, M6_3	British Museum
Yamato 74025	,52-1	NIPR
Yamato 75300	,51-3	NIPR
Yamato 8005	,51-1	
QUE 94535	16	MWG

sible, more than one section of a meteorite was examined to determine the extent of heterogeneity within and between the individual meteorites. All polished thin sections were examined with an optical microscope in transmitted and reflected light. Grain sizes were determined by measuring an average of twenty-five randomly selected grains in the more abundant fine-grained regions (matrix) of each section. While averages calculated from a small number of grains carry large standard deviations, they sufficiently illustrate the gross differences in grain sizes between individual winonaites (Fig. 2). Modal analyses of all thin sections were made in reflected light using a 40x objective. Olivine, orthopyroxene, and clinopyroxene were not distinguished but were collectively determined as mafic silicates. However, mafic silicates have been distinguished in previous studies (Graham et al., 1977; Prinz et al., 1980; King et al., 1981; Kimura et al., 1992), and the total mafic silicates and overall modes are similar to ours.

Mineral compositions were measured with a Cameca SX-50 electron microprobe operated at an accelerating voltage of 15 keV, a current of 20 nA, and a fully-focused beam. Well-known mineral standards were used, and the data were corrected using a company-supplied ZAF routine. The microprobe was also used to make X-ray image maps. For these maps, we used the same accelerating voltage and current, but increased the beam diameter to 20 μm to allow overlap of scan lines.

Unirradiated samples of Pontlyfni, Winona, and Mount Morris (Wisconsin), weighing from 34 to 44 mg were analyzed for trapped and cosmogenic noble gases He, Ne, Ar, Kr, and Xe using a VG model 3600 mass spectrometer. Additional samples, weighing from 23 to 30 mg, were used for ^{39}Ar-^{40}Ar age determinations on a different spectrometer. The latter samples were neutron-irradiated at Brookhaven National Laboratory together with four samples of the NL-25 hornblende age monitor. Argon was extracted from each sample by stepwise temperature release, and its isotopic composition was analyzed with a mass spectrometer. Irradiation constants (J values) for the individual samples were interpolated from known relative sample positions along a well-documented smooth neutron flux gradient. Uncertainties given for individual ^{39}Ar-^{40}Ar ages are derived from uncertainties in measured ratios, blank and reactor corrections, ^{37}Ar decay corrections, and J values. Absolute ages have an additional $\leq$0.5% uncertainty due to uncertainty in the accuracy of the age of the NL-25 hornblende.

4. RESULTS

Here, we discuss the textural, mineralogical, and compositional data on winonaites, as well as the ages of these rocks. Our work has primarily focused on examining the textural features and determining ^{39}Ar-^{40}Ar ages and trapped and cosmogenic noble gases. However, we will also compare our new mineralogical and compositional data with those in the literature and will be looking for possible correlations of all data with our textural observations.

4.1. Textures

Most winonaites exhibit equigranular textures with abundant triple junctions. Shock effects are very minor, with all winonaites studied classified as shock stage S1 (unshocked) or S2 (very weakly shocked; Stöffler et al., 1991), except for Y-75261, which is an impact-melt breccia. Variations in grain size are found both within and between winonaites (Table 2). Indeed, there seems to be a progression of the matrix grain size from the fine-grained Y-8005 to the coarse-grained Y-74025 (Fig. 2a,f). Metal and troilite textures also differ both within and between winonaites. We discuss the textures in order of increasing matrix grain size of the meteorites and have subdivided the winonaites into three categories based on similar textures: (1) Y-8005, Pontlyfni and QUE 94535; (2) Winona, Mount Morris (Wisconsin) and Y-75300; and (3) Tierra Blanca, Y-75305 and Y-74025. These categories are used only for descriptive purposes, allowing us to thoroughly describe the range of textural features found in the winonaites.

We had the opportunity to briefly examine thin sections of Y-75261 (,51-1 and ,51-2) and Y-75305 in the optical microscope at the National Institute of Polar Research. We find that Y-75305 is among the coarsest-grained winonaites, and we grouped it with Tierra Blanca and Y-74025. On the other hand, Y-75261 is an impact-melt breccia, with fine-grained clasts up to 3 mm in diameter consisting of silicates and finely distributed opaques with rare shock-melt pockets. The fine-grained melt matrix is composed of euhedral mafic silicates, a glassy to microcrystalline quench matrix and rounded Fe,Ni-FeS spheres. It is clear that Y-75261 is unlike any of the other winonaites. A detailed study of this meteorite will be required before its history and relationship to the winonaites can be fully interpreted.

4.1.1. Yamato 8005, Pontlyfni, and QUE 94535

Y-8005, Pontlyfni and QUE 94535 are the finest-grained winonaites, with average grain sizes of 55, 75, and 90 μm, respectively (Table 2). Pontlyfni and QUE 94535 do not exhibit the medium-grained, equigranular texture typical of Winona and other winonaites. Their textures are more similar to those of type 6 ordinary chondrites, exhibiting widely varying grain sizes, textures and mineralogy on a mm-scale. The dominant texture of Y-8005, Pontlyfni and QUE 94535 is a fine-grained aggregate of subrounded to anhedral mafic silicates, plagioclase, metal, and troilite (Fig. 2a,b,c). Some larger mafic silicates in these areas reach 0.5 mm in size. Metal and troilite are heterogeneously distributed, and metal commonly occurs as veins reaching 6 mm in length and up to 200 μm in width, or as large particles reaching 1 mm in maximum dimension. In Pontlyfni, graphite is frequently associated with the metal veins and, in two occurrences, we observed graphite fans reminiscent of those found in the Mundrabilla IAB iron (Buchwald, 1975). Veins of troilite were not observed in Pontlyfni, but the presence of physically isolated but optically continuous troilite over distances of 100 μm, as also found by Graham et al. (1977), suggests vein-like structures in three dimensions. Troilite veins are observed in QUE 94535. In Pontlyfni, troilite-rich areas up to several mm in diameter are found adjacent to the metal veins and these areas are virtually devoid of irregular, interstitial metal grains. In Y-8005, Pontlyfni and QUE 94535, metal, sulfide, and their weathering products also occur as micron-sized inclusions in mafic silicates, as also noted by Graham et al. (1977). These inclusions are randomly located in the silicates, unlike the dusty cores found in acapulcoites (e.g., Schultz et al., 1982).

Pontlyfni also has areas that are highly-enriched in plagioclase and calcic pyroxene. These areas are small, typically less than 500 μm in maximum dimension and relatively rare, certainly amounting to $<$1 vol%. They are very fine-grained, with typical grain sizes of 20–30 μm and have equigranular textures. These areas are irregularly shaped and appear to intrude the surrounding matrix. Figure 3a shows abundant plagioclase surrounding mafic minerals. Figure 3b is a merged Ca and Al X-ray dot map of a portion of the area in Fig. 3a, making possible clear distinction between plagioclase and calcic pyroxene.

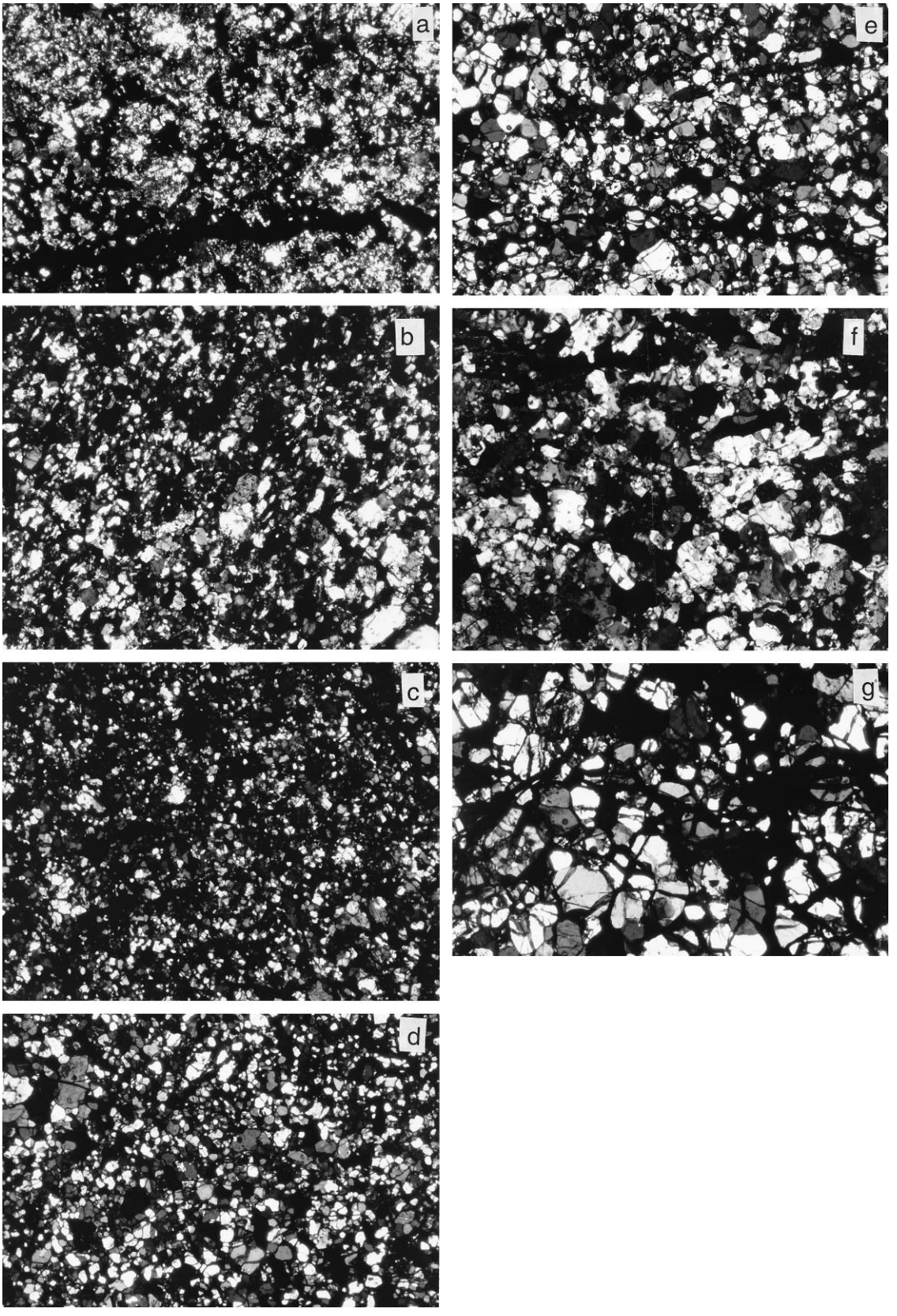

Fig. 2. Photomicrographs of winonaites illustrating range in grain sizes. Field of view = 2.5 mm. (a) Pontlyfni, (b) QUE 94535, (c) Yamato 8005, (d) Mount Morris (Wisconsin), (e) Winona, (f) Yamato 74025, (g) Tierra Blanca.

Table 2. Summary of petrologic and isotopic data of winonaites

	Olivine Fa		Low-Ca Px Fs	Wo		High-Ca Px Fs	Wo		Relict Chondrules	Shock Stage	Grain Size (μm)	2-Pyx temps (°C)	Fe,Ni-Fes Veins	$\Delta^{17}O$	^{39}Ar-^{40}Ar Ages (Ga)
WINONAITES EXAMINED IN THIS WORK															
Y-8005	1.2-2.1	(7,8)	2.0-2.2	1.5	(7,8)	1.5	46.1	(7)	No	S2	55		No	-0.53	
Pontlyfni	0.7-1.1	(1,2)	0.5-1.2	1.2-1.6	(1,2)	0.4-1.1	45.5-46.1	(1,2)	Yes	S2	75	975 (2)	Yes	-0.52	4.53-4.54
QUE 94535	1-3	(9)	1-2	--	(9)	--	--		No	S2	90		Yes	-0.67	
Mt. Morris (Wis.)	1.3-3.6	(1-4)	4.1	1.6	(3)	1.7	45.5	(4)	Yes	S1	125	930 (2)	Yes	-0.48	4.40
Winona	3.9-5.3	(1,3,4)	6.4-6.8	1.7-2.0	(1,3)	1.5-2.7	44.6-45.3	(4)	No	S1	110	1070(3)	Yes	-0.47	> 4.45
Y-75300	1.7-1.8	(1,6)	1.9-2.4	1.5-1.6	(1,6)	0.9-1.1	46.6-46.7	(1,6)	No	S2	100/300*	850 (6)	No	-0.48	
Y-74025	1.8	(6)	2.3	1.7	(6)	0.8	45.9	(6)	No	S1	230	940 (6)	No	-0.73	
Tierra Blanca	1.3	(5)	8.3	2.1	(5)	3.7	42.8	(5)	No	S2	190	1200(5)	No	-0.44	
WINONAITES NOT EXAMINED IN THIS WORK															
Y-75305	1.8	(6)	1.9	1.7	(6)	0.9	47.7	(6)				730 (6)		-0.53	
Y-75261	0.3	(7)	0.3	--	(7)	--	--							-0.40	

Data on relict chondrules, shock stage, grain size, presence of veins and ^{39}Ar-^{40}Ar ages from this work.
* fine-/coarse-grain sizes
References for 2-pyx temperatures indicate sources of data used in calculations.
Data on oxygen isotopic compositions from (10, 11)
References: (1) This Work (2) Graham et al., 1977 (3) Bild, 1977 (4) Prinz et al., 1980 (5) King et al., 1981 (6) Kimura et al., 1992 (7)Yanai and Kojima, 1995 (8)Yugami et al., 1996 (9) Mason, 1996 (10) Clayton and Mayeda, 1996 (11) R.N. Clayton, pers. comm., 1996

Graham et al. (1977) specifically noted the absence of chondrules or chondrule relicts in Pontlyfni, and we are unaware of any previous reports of chondrules or chondrule relicts in any of the winonaites. However, we have identified what appear to be relict chondrules ~700–800 μm in diameter in Pontlyfni (PTSs BM 1975.M6-2, -3). Several of these, while moderately recrystallized, preserve bars of pyroxene in a loosely radial pattern, suggesting that they are relict radiating pyroxene chondrules (Fig. 4a). The presence of radiating pyroxene chondrule relicts in a metamorphosed winonaite is not surprising, given that such chondrules are often prominent in type 6 ordinary chondrites, although porphyritic chondrules are the most common type (Gooding and Keil, 1981). In Pontlyfni, we also observe roughly circular to elliptical areas 1–3 mm in diameter that are possibly relict porphyritic chondrules. They are often prominent in appearance because of their differences in grain size and abundance of opaque minerals from the surrounding matrix (Fig. 4b).

4.1.2. Winona, Mount Morris (Wisconsin), and Yamato 75300

Winona, Mount Morris (Wisconsin) and Y-75300 have medium-grained equigranular textures, with average grain sizes ranging from 100–125 μm (Table 2). These meteorites (Fig. 2d,e) are coarser-grained than Pontlyfni and QUE 94535 (Fig. 2a-c). In many ways, QUE 94535 is transitional, exhibiting textural similarities to both Pontlyfni and Winona. In Mount Morris (Wisconsin) (USNM 1198-1), we discovered a fine-grained, roughly circular area 1 mm in diameter depleted in troilite and Fe,Ni-metal relative to the surrounding matrix. We interpret this area as a relict porphyritic chondrule, although, as in the case of Pontlyfni, this identification is ambiguous. Despite extensive terrestrial weathering of the finds Mount Morris (Wisconsin) and Winona, metal and troilite occur in Mount Morris (Wisconsin), Winona and Y-75300 dominantly as irregular, interstitial grains of ~100 μm in size, but also as inclusions in mafic silicates and as veins. Winona (PTSs UH 133, 195) contains veins of troilite with minor chromite that reach 7.5 mm in length and ~400 μm in width, as well as veins 9 mm in length and ~100 μm in width which are composed of discrete segments of Fe,Ni metal and troilite. In one case, a troilite-rich vein appears to cross-cut a metal-rich vein. Winona (USNM 854-1) and Mount Morris (Wisconsin) (UH 157, USNM 1198-1) also contain larger metal particles (4 × 1 mm), some of which are slightly elongate and may be cross-sections of veins.

Intermingled with the medium-grained areas (80–100 μm) which dominate these meteorites, are coarse-grained regions (average grain size 300–500 μm) which differ substantially in silicate mineralogy from the host. The coarse-grained regions occur as clumps of various sizes or, rarely, as veins and are sometimes located near patches or veins of Fe,Ni-metal, troilite, schreibersite and their weathering products. We found these in Winona (USNM 854-1) and Mount Morris (Wisconsin) (UH 157). X-ray dot maps and electron microprobe analyses reveal that these coarse-grained areas are rich in olivine, in sharp contrast to the host which is dominated by low-Ca pyroxene (Fig. 5).

Mount Morris (Wisconsin) and Y-75300 also exhibit coarse-grained regions, but these do not differ in silicate mineralogy from those of the more typical fine-grained regions. Y-75300 (,51-3) shows areas with two discrete grain sizes separated by a distinct, but not sharp, boundary (Kimura et al., 1992; Fig. 6a). The silicate mineralogy and mineral abundances of the two

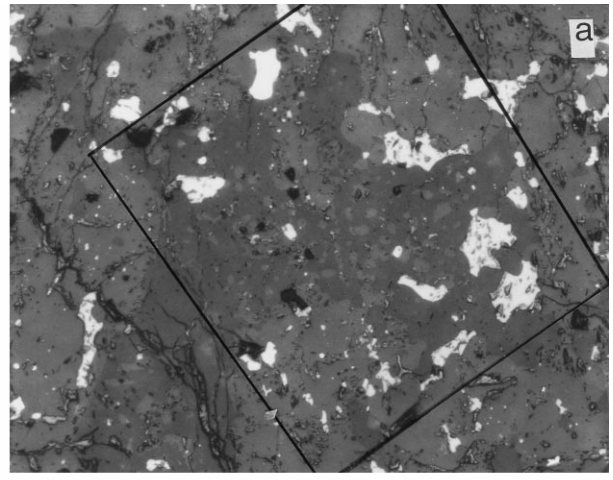

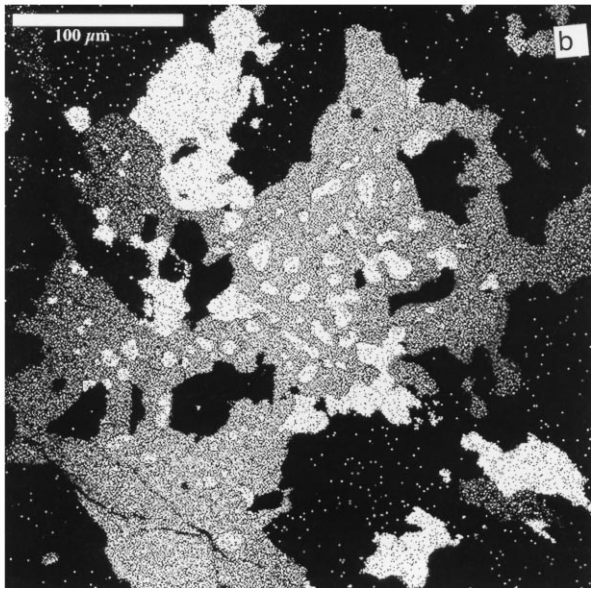

Fig. 3. Fine-grained, plagioclase-calcic pyroxene-rich areas of Pontlyfni. (a) Reflected light photomicrograph. Box indicates area shown in Fig. 3b. Scale bar = 100 μm. (b) Combined Al and Ca X-ray dot map of a portion of Fig. 3a. The area is dominated by calcic pyroxene (white) and plagioclase (medium gray). Olivine, low-Ca pyroxene, metal and troilite appear black. This distribution of plagioclase and calcic pyroxene may indicate silicate partial melting.

areas are nearly identical, with the exception that plagioclase is slightly more abundant (16.7 vs. 10.5 vol%) in the coarse-grained portion on a metal- and troilite-free basis. The fine-grained area has a granoblastic texture very similar to that of Winona and Mount Morris (Wisconsin), whereas the coarse-grained portion is essentially a coarser version of the same lithology. There is, however, a disparity in the amount of troilite between the fine-grained (10.0 vol%) and coarse-grained (27.5 vol%) areas (Kimura et al., 1992). Mount Morris (Wisconsin) (USNM 1198-1) exhibits coarser grains of olivine and pyroxene embedded in weathering products, metal and schreibersite (Fig. 6b).

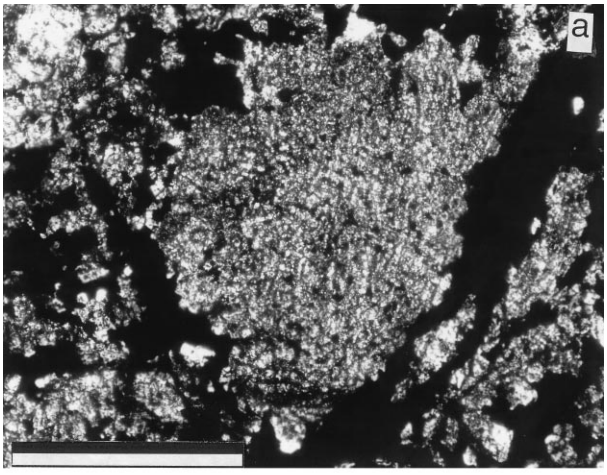

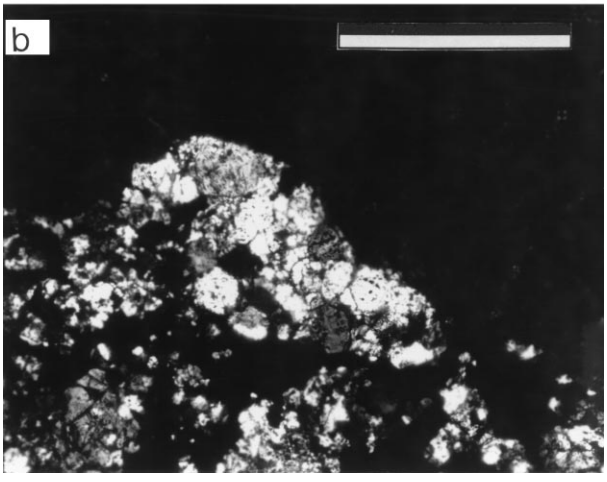

Fig. 4. Relict chondrules in Pontlyfni (PTS BM1975.M6-2). Scale bar = 500 μm. (a) Relict radiating pyroxene chondrule. (b) Relict porphyritic chondrule.

4.1.3. Tierra Blanca, Yamato 75305, and Yamato 74025

The coarsest-grained winonaites are Tierra Blanca and Yamato 74025 (Fig. 2f,g). Average grain sizes range from 190–230 μm (Table 2). Tierra Blanca has an equigranular texture with abundant 120° triple junctions, indicative of extensive solid-state recrystallization. Yamato 74025 is more variable in grain size and triple junctions are less abundant, suggesting less extensive solid-state recrystallization. No relict chondrules are observed in either meteorite. Metal, troilite, and their weathering products occur as interstitial, irregular grains. No metal or troilite veins are observed. Tierra Blanca does, however, contain veins of terrestrial weathering products which may have once been metal and/or troilite, although no elongate particles of metal or troilite are found in these weathering veins. Yamato 74025 contains very little metal (1.5–3.9 vol%; Table 3) or terrestrial weathering products. Tierra Blanca is very heavily weathered, with 26–31 vol% weathering products (Table 3).

Tierra Blanca contains large calcic pyroxenes which poikilitically enclose smaller olivine, plagioclase and low-Ca pyroxene grains. We have observed calcic pyroxenes up to 3 mm in size, although King et al. (1981) observed calcic pyroxenes up

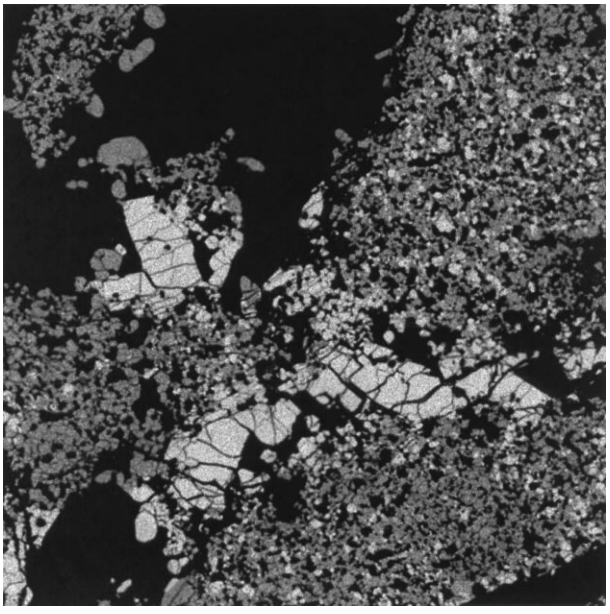

Fig. 5. Mg X-ray dot map of Mount Morris (Wisconsin) (UH 157), illustrating the correlation between grain size and mineral composition. Light gray indicates high Mg (olivine), medium gray indicates a moderate amount of Mg (low-Ca pyroxene), and dark gray indicates low Mg (calcic pyroxene). Coarse-grained areas are predominantly olivine. Field of view = ~5 mm.

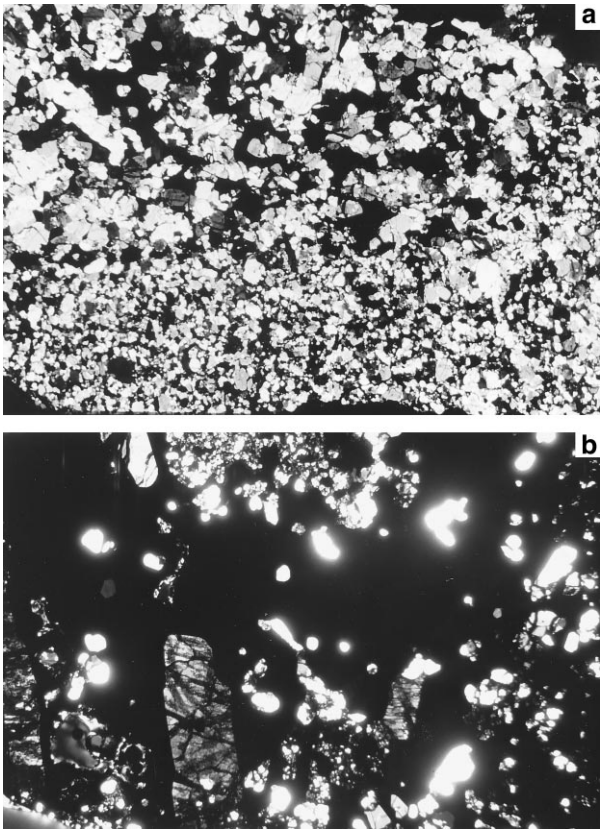

Fig. 6. Photomicrographs of coarse-grained/fine-grained regions in winonaites in transmitted light, crossed polars: (a) Boundary between coarse and fine grains in Y-75300. Field of view = ~5 mm. (b) Coarse-grained olivines and pyroxenes embedded in metal, schreibersite, troilite, and their weathering products in Mount Morris (Wisconsin). Field of view = ~5 mm.

to 9 mm in size. Fig. 7 is a merged Al and Mg X-ray dot map of Tierra Blanca. Calcic pyroxene occurs only as these large, poikilitic grains and shows no preferential association with plagioclase, unlike in Pontlyfni (Figs. 3a,b). Plagioclase is distributed randomly throughout the section. Also observed in this image, but not evident optically, are clumps of olivine grains similar to those found in Winona and Mount Morris (Wisconsin). One olivine clump appears to be associated with the larger calcic pyroxene grain.

4.2. Modal Composition and Mineralogy

Winonaites contain low-Ca pyroxene, olivine, calcic pyroxene, plagioclase, Fe,Ni-metal, and troilite as major phases, with chromite, daubreélite, alabandite, schreibersite, graphite, K-feldspar, and apatite occurring as accessory phases (Prinz et al., 1980; Kimura et al., 1992). The modal compositions (in vol%) of all the winonaites studied are given in Table 3, and these are broadly similar to those of chondrites. Previous workers have shown that low-Ca pyroxene is the dominant mafic silicate, in contrast to ordinary chondrites, where olivine dominates (McSween et al., 1991). This is consistent with the more reduced nature of winonaites compared to ordinary chondrites, as discussed below. The roughly chondritic plagioclase contents are a second interesting feature. Individual winonaites vary from 6.3–14.0 vol% (Table 3) in plagioclase content, although most are close to 10%, the approximate abundance in ordinary chondrites (Van Schmus and Ribbe, 1968; McSween et al., 1991). The amount of calcic pyroxene varies among winonaites, with Tierra Blanca (6 vol%; King et al., 1981) and Y-74025 (7 vol%; Kimura et al., 1992) being the most calcic pyroxene-rich members. The other winonaites typically have ≤3 vol% (Graham et al., 1977; Prinz et al., 1980). Extensive terrestrial weathering has introduced considerable uncertainties in metal and troilite contents of some winonaites [Winona, Mount Morris (Wisconsin), Tierra Blanca]. However, relatively unweathered winonaites such as Pontlyfni and Yamato 74025 have metal contents ranging from 1.5 to 12.3 vol% and troilite contents ranging from 9.1 to 19.9 vol% (Table 3). This suggests that the winonaite parent body was relatively heterogeneous as far as these minerals are concerned.

Contents of accessory mineral phases which are common in enstatite meteorites and which are indicative of highly-reducing conditions, such as daubreélite ($FeCr_2S_4$) and alabandite (MnS), vary dramatically. For example, daubreélite contents vary from 0.2 to 1.0 vol% in Mount Morris (Wisconsin), Pontlyfni, Y-74025 and Y-75300 (the more highly-reduced winonaites), whereas the more oxidized Tierra Blanca and Winona contain 0.09–0.10 vol% chromite, which is rare or absent in the remaining winonaites.

4.3. Silicate Compositions

Compositions of mafic silicates range considerably among winonaites, but generally are quite reduced and intermediate between E ($Fa_{0.0-9.0}$;$Fs_{0.03-22.0}$; Lusby et al, 1987; Keil, 1968;

Table 3. Modal compositions of winonaites (in vol%)

Meteorite	Ref.	Mafics*	Plag.	Troilite	Fe,Ni	W.P.	Chr.	Daub.	Schreib.	Graph.
Pontlyfni										
M6.2	(1)	57.9	9.5	18.2	9.5	3.1	0.06	0.67	1.04	tr
M6.3	(1)	53.2	8.7	19.9	12.3	4.6	-	0.8	0.2	tr
QUE 94535										
16	(1)	64.0	13.8	6.0	2.6	13.7	-	0.08	-	tr
Winona										
UH 133	(1)	66.1	13.3	5.1	1.8	13.4	0.10	-	-	-
UH 195	(1)	68.2	12.2	6.1	2.3	11.2	0.10	-	-	-
USNM 854-1	(1)	64.7	14.0	6.3	2.2	12.4	0.10	-	-	-
Mt. Morris (Wis.)										
UH 157	(1)	65.5	9.4	5.8	3.5	15.1	-	0.2	-	tr
USNM 1198-2	(1)	65.7	11.5	8.7	0.2	13.2	-	0.3	-	-
Y-75300										
,51-2 (coarse)	(3)	56.0	11.2	27.5	3.8	-	-	1.0	0.4	-
,51-2 (fine)	(3)	79.4	9.3	10.0	0.7	-	-	0.4	0.2	-
,51-3 (coarse)	(1)	57.8	13.3	15.2	0.4	12.7	-	0.7	-	-
,51-3 (fine)	(1)	75.2	12.2	7.5	-	5.1	-	-	-	-
Y-74025										
,52-1	(1)	71.5	12.7	9.1	1.5	4.9	-	0.3	-	-
,52-2	(3)	72.7	8.3	13.5	3.9	-	-	0.7	0.9	-
Tierra Blanca										
King section‡	(2)	85.0	14.0	0.7	0.2	-	-	-	0.1	-
M-3,1	(1)	63.1	8.8	1.44	-	26.2	-	-	-	0.56
M-3,2	(1)	61.6	6.3	0.17	0.09	31.8	0.09	-	-	-
Y-75305										
,52-2	(3)	54.0	8.3	9.2	27.0	-	0.2	1.0	0.3	-
Y-8005										
,51-3	(4)	52.9	8.1	8.3	12.5	16.8	-	0.7	0.6	-

* Mafic silicates were not distinguished and include olivine, orthopyroxene and clinopyroxene
‡ Weathering products were not included in the mode given.
References: (1) This Work. (2) King *et.al.* (1981). (3) Kimura *et.al.* (1992) (4) Yugami et al. (1996).
- = not observed.
tr = trace.

Weisberg et al., 1995) and H (Fa_{16-20};Fs_{15-18}; Dodd, 1981; Gomes and Keil, 1980) chondrites (Table 4). Olivine compositions range from $Fa_{0.3}$ (Y-75261) to $Fa_{4.6}$ (Winona) and low-Ca pyroxene compositions from $Fs_{0.3}$ (Y-75261) to $Fs_{8.3}$ (Tierra Blanca; Table 2 and references therein). A plot of Fa in olivine vs. Fs in low-Ca pyroxene (Fig. 8) reveals that, with the exception of QUE 94535, Fa values are lower than, or equal to, Fs values for each meteorite, indicative of reduction. At least two winonaites exhibit differences in mineral compositions which can be correlated with textural settings. Mount Morris (Wisconsin) (UH 157) exhibits a slight difference in Fe content between the coarse-grained olivines ($Fa_{3.6 \pm 0.1}$) and the matrix olivines ($Fa_{3.1 \pm 0.05}$). In Tierra Blanca, both olivines and low-Ca pyroxenes contained in large poikilitic calcic pyroxenes are more FeO-rich than those in the matrix (King et al., 1981). Calcic pyroxene is diopside, with compositions ranging from $Fs_{0.8}Wo_{45.9}$ (Y-74025) to $Fs_{3.7}Wo_{42.8}$ (Tierra Blanca; Table 2). Plagioclase compositions range from $An_{7.7}$ (Pontlyfni) to $An_{25.1}$ (Y-75300) and are found to be heterogeneous throughout single sections (King et al., 1981; this work), with ranges of An_{7-9} in Pontlyfni and An_{12-15} in Tierra Blanca sections we examined, and An_{13-25} in Tierra Blanca sections examined by King et al. (1981). Although there is some variation in mineral compositions on a thin section scale, most authors have either noted that the minerals are homogeneous (Kimura et al., 1992) or not specifically discussed possible zoning (e.g., Graham et al., 1977; Davis et al., 1977; King et al., 1981). Yugami et al. (1996) noted normal FeO zoning in both olivine and low-Ca pyroxene in Y-8005, but did not comment on its magnitude. We have observed only very slight reverse zoning in olivine of Winona, with rims typically 0.1 mol% Fa lower than cores, and no zoning of FeO in Y-8005.

4.4. Equilibration Temperatures

Two-pyroxene equilibration temperatures were calculated for these rocks from the compositions of coexisting low-Ca and high-Ca pyroxenes. Calculated temperatures range from 730° (Y-75305) to 1200°C (Tierra Blanca; Table 2), using the transfer equations of Kretz (1982). Kimura et al. (1992) used the method of Lindsley and Anderson (1983) and calculated temperatures in the range of 800–900°C for Y-74025,

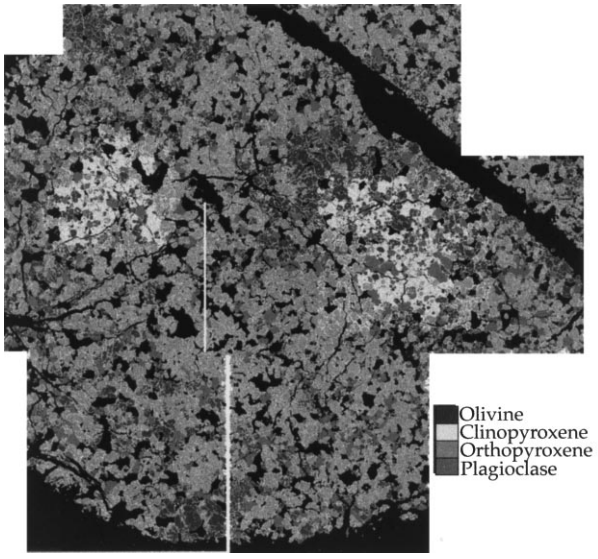

Fig. 7. Merged Mg and Al X-ray dot map. This map highlights two poikilitic calcic pyroxene grains (white) as well as the distribution of orthopyroxene (light gray), plagioclase (medium gray) and olivine (dark gray) in Tierra Blanca. There is no significant difference in texture or composition between plagioclase grains that are poikilitically enclosed and those in the matrix. The absence of textures indicating melting suggests that the poikilitic calcic pyroxenes formed by solid state reaction during metamorphism. Maximum width = ~15 mm.

Y-75300, and Y-75305, within the range of our calculated temperatures. These temperatures are consistent with the highly metamorphosed textures seen in winonaites, although uncertainties due to pyroxene compositional variability may be significant. For example, selected two-pyroxene pairs in Pontlyfni yield temperatures that vary by ~80°C (980–1060°C). In addition, Kretz (1982) cites an uncertainty of ±60°C resulting from precision and accuracy errors. Thus, total errors may exceed 100°C. Despite these uncertainties, it is interesting to note that Tierra Blanca, which has the largest grain size, has the highest two-pyroxene equilibration temperature (1200°C).

4.5. Bulk Major and Trace Element Compositions

Although we present no new data on bulk major or trace element compositions, these data are important to understanding the genesis of this group, and we, therefore, briefly review previous work here. Partial or complete bulk major element compositions of winonaites have been determined for Tierra Blanca (King et al., 1981; Kallemeyn and Wasson, 1985), Winona (Mason and Jarosewich, 1967), Mount Morris (Wisconsin) and Pontlyfni (Graham et al., 1977), Y-74025 (Kimura et al., 1992) and Y-75300 (Yamamoto et al., 1991). Large uncertainties exist in bulk compositions of some winonaites due to extensive terrestrial weathering. As a general rule, the bulk major element compositions are similar to those of chondrites, as noted by King et al. (1981) in discussing Tierra Blanca and Winona. Graham et al. (1977) noted that Ca/Al ratios in winonaites are more variable than expected for ordinary chondrites and that S/Si ratios are low in Winona compared to Pontlyfni and Mount Morris (Wisconsin). Kallemeyn and Wasson (1985) attribute at least some deviations from chondritic values to unrepresentative sampling. Despite uncer-

Table 4. Olivine and pyroxene compositions of winonaites (this work).

	Olivine				Orthopyroxene			Clinopyroxene
	Winona	Mt. Morris (Wis.)	Pontlyfni	Y-75300	Winona	Pontlyfni	Y-75300	Pontlyfni
SiO_2	41.4	41.8	42.7	42.1	58.1	59.2	59.37	55. 0
	(0.36)	*(0.17)*	*(0.24)*	*(0.19)*	*(0.25)*	*(0.24)*	*(0.41)*	*(0.34)*
TiO_2	n.d.	n.d.	n.d.	n.d.	n.d.	b.d.	n.d.	0.36
								(0.28)
Al_2O_3	n.d.	n.d.	n.d.	n.d.	n.d.	0.34	n.d.	0.58
						(0.15)		(0.16)
Cr_2O_3	n.d.	n.d.	n.d.	n.d.	n.d.	b.d.	n.d.	b.d.
FeO	4.85	3.35	0.77	1.69	4.53	0.33	1.69	0.36
	(0.45)	*(0.28)*	*(0.25)*	*(0.30)*	*(0.12)*	*(0.18)*	*(0.61)*	*(0.28)*
MnO	0.33	0.26	0.16	0.24	0.39	b.d.	0.22	b.d.
	(0.03)	*(0.03)*	*(0.03)*	*(0.04)*	(0.02)		(0.03)	
MgO	53.4	54.8	56.9	55.9	36.7	39.4	37.8	19.5
	(0.43)	*(0.33)*	*(0.20)*	*(0.10)*	*(0.14)*	*(0.24)*	*(0.38)*	*(0.20)*
CaO	b.d.	b.d.	b.d.	b.d.	0.97	0.76	0.89	23.4
					(0.07)	*(0.18)*	*(0.39)*	*(0.43)*
Na_2O	n.d.	n.d.	n.d.	n.d.	n.d.	b.d.	n.d.	0.35
								(0.08)
Total	100.02	100.22	100.56	99.90	100.67	100.12	99.94	99.57
N	43	20	26	13	16	16	10	14
Fa	4.9	3.3	0.8	1.7	--	--	--	--
Fs	--	--	--	--	6.4	0.5	2.4	0.6
Wo	--	--	--	--	1.7	1.4	1.6	46.1

N=Number of analyses; b.d. = below detection limit; n.d. = not determined
Italicized figures are 1σ of compositional variability.

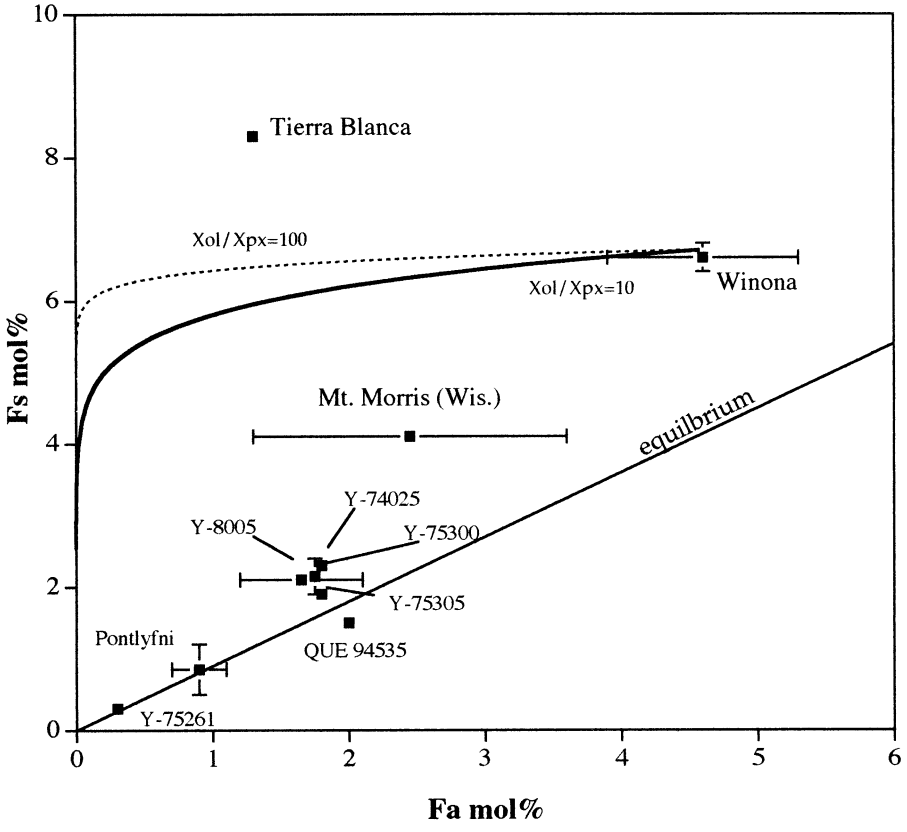

Fig. 8. Fa in olivine vs. Fs in low-Ca pyroxene in the winonaites. If reduction were due to metamorphism, the Fa and Fs values would follow the calculated X_{ol}/X_{px} curves (see Discussion) on the plot, since diffusive reduction of FeO occurs more rapidly in olivine than in low-Ca pyroxene. We observe a nearly linear trend, distinct from an equilibrium trend, which indicates that the reduced mineral compositions are more likely due to heterogeneity in the precursor chondrite. Bars illustrate ranges in average Fa and/or Fs reported by different investigators for individual winonaites (they do not represent errors in any single measurement of Fa or Fs).

tainties due to weathering and sampling, bulk major element compositions indicate considerable variability between winonaites in plagioclase, metal, and sulfide abundances, a feature we also observed in the modal analyses (Table 3), suggesting heterogeneity in these minerals in the winonaite parent body.

Bulk trace element contents including the REE have also been measured for Winona (Prinz et al., 1980), Pontlyfni (Davis et al., 1977; Kallemeyn, 1996), Tierra Blanca (Kallemeyn and Wasson, 1985), Y-74025 (Kimura et al., 1992) and Y-75300 (Yamamoto et al., 1991). While the data show considerable variation in both the shape of the REE abundance patterns and in absolute abundances, some similarities are noted. In both Winona and Y-74025, multiple samples were analyzed yielding two patterns, one negatively bowed with a positive Eu anomaly and the other positively bowed with a negative Eu anomaly. Kimura et al. (1992) performed a mass-weighted mean of their two samples of Y-74025, producing an essentially unfractionated pattern. Analyses of Tierra Blanca and Y-75300 reveal the same negatively bowed pattern with a positive Eu anomaly found for individual splits of Winona and Y-74025. Pontlyfni's pattern is similar, but without the relative heavy REE enrichment found in Tierra Blanca and Y-75300. Kallemeyn and Wasson (1985) noted that these bowed-patterns with Eu anomalies can be readily explained by an increase or depletion of phosphates relative to a chondritic precursor. While some authors have favored igneous fractionation (e.g., melting and migration of plagioclase-phosphate-rich melts; Davis et al., 1977), it is impossible to rule out unrepresentative sampling of these coarse-grained rocks, as noted by Kallemeyn and Wasson (1985).

4.6. Cooling Rates

We have not been able to determine metallographic cooling rates for winonaites due to their highly weathered nature or small metal grain sizes of the samples studied. A metallographic cooling rate has previously been determined for Winona by Kothari et al. (1981), who argued for a cooling rate of ~200°C/Myr at a temperature of 530°C. With only nine metal grains analyzed, these authors estimated an uncertainty in this rate of up to 50%.

4.7. ^{39}Ar-^{40}Ar Chronology

Samples of Winona, Pontlyfni, and Mount Morris (Wisconsin) were dated using the ^{39}Ar-^{40}Ar method (Appendix A). Calculated ^{39}Ar-^{40}Ar ages and K/Ca ratios as a function of fractional release for stepwise temperature extractions of the

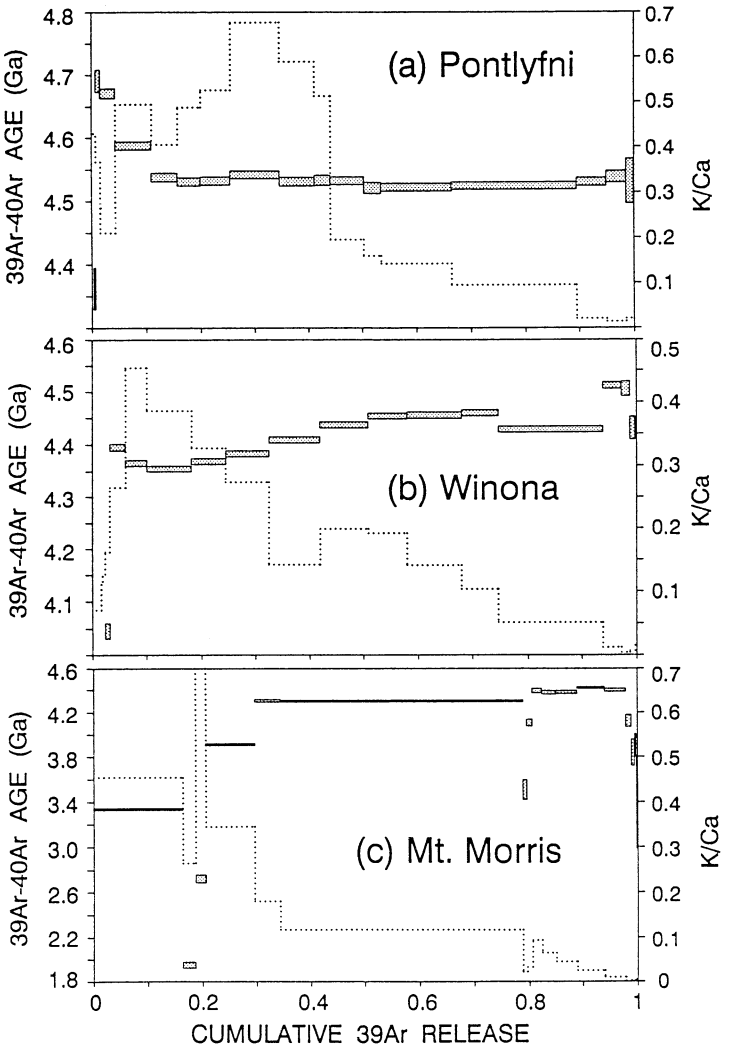

Fig. 9. ^{39}Ar-^{40}Ar ages (rectangles) and K/Ca ratios (dotted lines) as a function of cumulative release of ^{39}Ar for stepwise temperature extractions of Pontlyfni (a), Winona (b), and Mount Morris (Wisconsin) (c). Individual age uncertainties are indicated by the widths of the rectangles and include all analytical uncertainties, but not that associated with the age of the hornblende age monitor.

three winonaites are shown in Fig. 9a-c. The determined K concentrations for our samples of Pontlyfni, Winona, and Mount Morris (Wisconsin) are 715, 900, and 328 ppm, respectively; Ca concentrations are 0.81, 1.6, and 0.99%, respectively. Although uncertainties associated with individual ages are relatively small, derivation of the preferred ^{39}Ar-^{40}Ar age for these samples depends on interpretation of complex Ar release profiles, as is discussed below.

Pontlyfni, a fall, shows the simplest Ar release pattern. Thirteen extractions (750–1550°C), releasing 89% of the total ^{39}Ar, give a constant age of 4.531 $\pm$ 0.006 Ga (1σ). The first five extractions, releasing 11% of the ^{39}Ar, all give ages higher than the plateau age. Thus, the total age of all extractions is 4.538 Ga. Although the first (400°C) extraction certainly released absorbed terrestrial ^{40}Ar, it is unlikely that terrestrial Ar contamination is the sole cause for the higher ages of other low-temperature extractions. A small air-Ar correction has been applied to the 400–600°C temperature data shown in Fig. 9, but the peak in Ar-Ar ages remains after this correction. This applied correction is based on two assumptions: that the cosmogenic ^{36}Ar/^{37}Ar ratio produced from space exposure to cosmic rays is relatively constant with extraction temperature, and that any excess ^{36}Ar above this constant ratio and released at lower extraction temperature is due to terrestrial Ar contamination. This air-Ar correction is probably the maximum that should be applied because it forces the age of the 400°C extract to near zero.

From the above considerations, we conclude that the higher Pontlyfni ages observed at lower temperatures represent recoil loss of ^{39}Ar during neutron irradiation (e.g., Huneke and Smith, 1976). Although no extraction temperature shows a significantly lowered age indicative of implantation of this recoil ^{39}Ar, recoil capture may have affected part of the age plateau. The abrupt decrease in the K/Ca ratio and the minimum in the rate of degassing of ^{39}Ar at ~50% ^{39}Ar release (Fig. 9a) strongly indicate that K occurs in different phases with quite

different Ar degassing properties. We note that the mean age of the high K/Ca phase releasing Ar in the first degassing peak (seven extractions, 750–925°C) is 4.535 ± 0.004 Ga, whereas the mean age of the low K/Ca phase releasing Ar in the second degassing peak (six extractions, 1000–1550°C) is slightly lower at 4.525 ± 0.007 Ga. This age difference could be consistent with the higher temperature phase having received some of the recoiled ^{39}Ar, which then lowered its apparent age. Mass balance considerations indicate that the amount of ^{39}Ar that recoiled out of the first ~11% of the ^{39}Ar release spectrum approximately equals (within a factor of two) the age depression suggested by the last ~50% of the ^{39}Ar release. This interpretation suggests that the total ^{39}Ar-^{40}Ar age of 4.538 Ga is a better measure of the closure time of this isotopic system. However, we cannot completely exclude the possibility that part of the recoiled ^{39}Ar was completely lost from the sample, and that the average plateau age is a better measure of the time of Ar closure. Thus, we conclude that the ^{39}Ar-^{40}Ar age of Pontlyfni closed around 4.530–4.535 Ga ago and that the rock experienced no significant thermal heating after that time. Turner et al. (1978) reported generally similar ^{39}Ar-^{40}Ar age data for Pontlyfni (although of lesser precision). Five extractions (releasing ~75% of the ^{39}Ar) define a "plateau" age of ~4.53 Ga, in excellent agreement with the age reported here. In addition, Kennedy (1981) reported ^{129}I/^{129}Xe data for an irradiated sample of Pontlyfni. Although the data were not reduced, they suggest a formation interval similar to that for several chondrites.

The Ar release spectrum of Winona (Fig. 9b) shows slowly increasing ages across part of the ^{39}Ar release. Variations in some individual ages outside analytical age uncertainty may reflect textural differences observed in Winona. The first ~3% of the ^{39}Ar release gives ages of ~2.8–4.0 Ga and indicates post formational ^{40}Ar loss from a phase with lower K/Ca, possibly due to grain surface weathering. Unlike Pontlyfni, more gradual changes in the K/Ca ratio and lack of separation of the rate of ^{39}Ar release into distinct peaks for Winona indicate overlapping Ar release from different K-bearing phases. Only the first extraction suggests significant terrestrial Ar contamination, and the other extractions have received no correction for air-Ar. Two extractions at ~3–11% ^{39}Ar release show very slightly higher ages that might suggest ^{39}Ar recoil, but the amount of such recoil would be small. The average age of fourteen extractions (675–1350°C) defining the sloped "plateau" is 4.42 ± 0.05 Ga. The last ~50% of the ^{39}Ar release gives an average age of 4.45 ± 0.03 Ga. The highest age of ~4.51 Ga is shown by two high temperature extractions (1150 and 1250°C). Kothari et al. (1981) reported fission track ages of 4.50 to 4.53 Ga for Winona. The existence of a sloped Ar-Ar age profile suggests one of two possible explanations. Winona may have formed initially at > 4.45 Ga and cooled slowly over ~100 Ma such that different phases experienced closure to Ar diffusion at different times. This would imply very deep burial during cooling in order to maintain a sufficiently high temperature to cause Ar to be lost. Alternatively, the rock may have initially formed at > 4.45 Ga and experienced a secondary degassing event ~4.3 Ga ago which caused loss of ^{40}Ar from some phases. This explanation might be consistent with impact and surface brecciation. Both explanations suggest that Winona formed prior to 4.45 Ga ago.

The Ar release spectrum of Mount Morris (Wisconsin; Fig. 9c) is the most complex of the three. The 775°C extraction was accidentally overheated by 150°C for ~3 min, before the temperature was returned to 775°C for an additional ~40 min. This probably caused the relatively large ^{39}Ar release at this temperature and the very small ^{39}Ar releases at the two subsequent extractions. The first ~25% of the ^{39}Ar release indicates significant amounts of ^{40}Ar loss long after the rock formed. The very first (400°C) extraction released a relatively large amount of ^{39}Ar and also gives evidence of considerable contamination by terrestrial Ar. (No air-Ar correction was made to the data shown in Fig. 9). This low-temperature Ar could represent weathering of some grain surfaces, with possible deposition of K and loss of radiogenic ^{40}Ar. Both the K/Ca ratios and the rate of release of ^{39}Ar as a function of extraction temperature suggest distinct K-bearing phases with different Ar diffusion properties. The four highest temperature extractions (releasing the last ~2% of the ^{39}Ar) show lower ages suggestive of implantation of small amounts of recoiled ^{39}Ar. A lower limit to the ^{39}Ar-^{40}Ar closure age of Mount Morris (Wisconsin) probably is given by the constant age of 4.40 ± 0.02 Ga shown by five extractions releasing ~83–98% of the ^{39}Ar. This age might represent the time of closure of the ^{39}Ar-^{40}Ar chronometer after initial meteorite formation or, more likely, the time of an early thermal event that reset the Ar-Ar age.

4.8. Cosmogenic and Trapped Noble Gases

We analyzed unirradiated samples of Winona, Pontlyfni, and Mount Morris (Wisconsin) to characterize any trapped noble gases and those species produced by cosmic rays during space exposure (Table 5). Gases were extracted in a low temperature step (two steps for Winona) and a melt extraction (1550°C) in order to separate any adsorbed terrestrial atmospheric gases. The isotopic compositions of Kr and Xe in these low temperature steps closely resemble those of terrestrial air, and the xenon isotopic compositions given are those measured at the melt extraction. Only a small fraction of the total Ne and Ar were released at low temperature, with the Ne being mostly cosmogenic in composition, but the Ar appearing to be largely trapped or terrestrial in composition.

The ^{22}Ne/^{21}Ne ratios of ~1.08 for Pontlyfni and Winona suggest moderate cosmic ray shielding, whereas the ratio of ~1.03 for Mount Morris (Wisconsin) seems unusually low, even for the case of very large shielding. The low ^{3}He/^{21}Ne ratios for all three meteorites are consistent with moderately large shielding. We assume that our samples of these winonaites had the same chemical composition as ordinary chondrites, and we utilized the cosmogenic production rates for ordinary chondrites given by Eugster (1988) to calculate the ^{3}He, ^{21}Ne and ^{38}Ar exposure ages given in Table 5. These three ages for Mount Morris (Wisconsin) are all similar, with an average value of ~20 Myr. An ^{38}Ar age of ~18 Myr is calculated assuming that trapped ^{36}Ar/^{38}Ar = 5.32 in Mount Morris (Wisconsin). If we assume that trapped ^{36}Ar/^{38}Ar has the "subsolar" ratio of 5.46 measured for enstatite chondrites (Crabb and Anders, 1981; see later discussion), the ^{38}Ar exposure age becomes ~22 Myr. The calculated exposure ages for Pontlyfni and Winona show more scatter, but suggest considerably older ages of ~60–80 Myr. It is conceivable that

Table 5. Trapped and cosmogenic noble gases* in three winonaites.

Meteorite		Mt. Morris			Pontlyfni			Winona			
Temperature °C		400	1550	Total	350	1550	Total	400	450	1550	Total
^{3}He	10^{-8}	2.13	31.4	33.5	10.5	91.5	102	57.1	19.7	39.7	116.5
^{4}He	10^{-6}	1.04	7.22	8.27	2.94	22.7	25.7	63.43	3.50	5.05	12.0
^{20}Ne	10^{-8}	3.76	8.76	12.5	0.77	19.7	20.5	1.01	0.63	10.63	12.27
^{21}Ne	10^{-8}	0.59	9.69	10.28	0.52	21.8	22.3	0.15	0.14	11.34	11.62
^{22}Ne	10^{-8}	0.94	10.0	10.94	0.79	23.2	24.0	0.27	0.21	12.32	12.81
Cos. ^{21}Ne	10^{-8}			10.27			22.3				11.6
Cos. ^{22}Ne/^{21}Ne			1.029 ±0.001			1.077±0.001				1.087 ±0.001	
^{3}He/^{21}Ne				3.26	20.2	4.2	4.6		145	3.5	10.0
^{36}Ar	10^{-8}	0.23	63.4	63.6	0.68	8.83	9.51	0.30	0.02	13.31	13.62
^{38}Ar	10^{-8}	0.04	12.4	12.4	0.16	5.03	5.19	0.08	0.07	4.80	4.95
Cos. ^{38}Ar	10^{-8}			0.81			3.93				2.79
Trapped ^{36}Ar	10^{-8}			62.1			6.83				11.7
^{40}Ar	10^{-6}	0.65	19.0	19.6	1.98	56.7	58.7	1.67	1.76	52.33	55.76
^{84}Kr	10^{-10}	3.84	12.3	16.1	1.72	2.39	4.10	1.36		4.68	6.04
^{132}Xe	10^{-10}	0.58	9.56	10.1	0.38	1.88	2.26	0.23		2.73	2.96
Cos. ^{126}Xe	10^{-12}			0.69			2.33				0.30
Excess ^{129}Xe	10^{-10}			1.37			2.80				7.75
^{129}Xe/^{132}Xe			1.196 ±0.0043			2.46 ±0.025				3.877 ±0.028	
^{134}Xe/^{132}Xe			0.3735 ±0.0015			0.3814 ±0.0043				0.3830 ±0.003	
^{136}Xe/^{132}Xe			0.3095 ±0.0011			0.3202 ±0.0060				0.3220 ±0.0034	
Exposure Ages in Myr:**											
^{3}He				20			63				72
^{21}Ne				22			57				31
^{38}Ar				18-22			89				64

*Gas concentrations are in units of cm^{3}STP/g and have uncertainties of <5% for Ar and <10% for other gases. Gas concentrations are to be multiplied by the exponent in column two.

**Cosmogenic production rates used are those for L-chondrities given by Eugster (1988) and Eugster et al. (1993).

Pontlyfni and Winona have the same exposure age: The older ^{38}Ar age for Pontlyfni and the younger ^{21}Ne age for Winona may reflect nonchondritic major element abundances for our samples. Niemeyer (1979) reported ^{38}Ar exposure ages of ~130–700 Myr for silicates from four IAB iron meteorites. These ages are all older than exposure ages for the three winonaites reported here. This suggests that space exposure of winonaites was initiated by younger impact events than those for IAB irons, and that winonaites survive for shorter times in space. Previous noble gas analyses of winonaites apparently have not been reported, except for one older analysis of Winona (analysis by T. Kirsten, reported by Mason and Jarosewich, 1967) that gave slightly lower ^{3}He but substantially larger ^{21}Ne, compared to our analysis.

These three winonaites, especially Mount Morris (Wisconsin), contain significant concentrations of trapped Ar, Kr, and Xe with solar-like characteristics. Assuming that the relatively small fraction of the total ^{36}Ar released at low extraction temperatures is a trapped component and not terrestrial contamination, the calculated concentrations of trapped ^{36}Ar are $\sim 7\text{–}62 \times 10^{-8}$ cm^{3}STP/g (Table 5). By comparison, this is similar to trapped ^{36}Ar concentrations observed in several carbonaceous chondrites (Zähringer, 1968; Mazor et al., 1970) and in irradiated silicates from three IAB iron meteorites (Niemeyer, 1979). Concentrations of trapped Kr and Xe in winonaites, however, are better given by the melt extractions alone, because the low temperature extractions contain a significant fraction of terrestrial-like gas. These three winonaites contain no trapped He and Ne, so it is unlikely that these trapped gases simply represent solar wind gas implanted into dispersed fine material, such as occurs in lunar surface soils and solar gas-rich meteorites.

5. DISCUSSION

Clues to the history of the winonaite parent body can be inferred from our and previously published data, as summarized above. We are mostly interested in the following six aspects of this history: (1) the nature of the chondritic precursor material, (2) the heating history, particularly evidence for partial melting, as deduced from petrology and major element composition, (3) the impact brecciation history, inferred from textural features, (4) the metamorphic and cooling history, which affected mineral compositions and textures, (5) significance of trapped noble gases, and (6) comparison of ages of winonaites with those of silicate inclusions in IAB irons.

5.1. Precursor Chondritic Material

The chondritic nature of the precursor material of the winonaite body is suggested by the roughly chondritic bulk elemental compositions and mineralogy of the winonaites, as well as the presence of what appear to be relict chondrules in Pontlyfni and Mount Morris (Wisconsin). However, the composition of this precursor material is unlike that of any of the known classes of chondrites. Mineral compositions are intermediate between E and H chondrites, and the oxygen isotopic compositions are unlike any group of known chondrites (Clayton and Mayeda, 1996). Further, at least some winonaites contain a solar-like component of noble gases (discussed below) that is similar to what is found in E chondrites. While it seems clear that winonaites formed from a chondritic precursor material, classification as chondrites, as suggested by Kallemeyn and Wasson (1985), is not warranted, given the extensive metamorphism and partial melting these rocks have experienced, as discussed below.

We suggest that the winonaites formed from heterogeneous chondritic precursors. There is a correlation between mineral compositions (Fa, Fs) and oxygen isotopic compositions ($\delta^{17}O$) in ureilites (Clayton and Mayeda, 1988) and lodranites (McCoy et al., 1997a) that is taken as evidence of primary heterogeneity in the precursors of these groups. No such correlation exists in the winonaites. However, a correlation does exist between mineral compositions and mineralogy of the winonaites. More FeO-rich ($Fs_{6.8}$-$Fs_{8.3}$) winonaites contain oxidized accessory minerals such as chromite ($FeCr_2O_4$), whereas those with more FeO-poor minerals ($Fs_{0.3}$-$Fs_{4.1}$) contain reduced accessory minerals such as daubreélite ($FeCr_2S_4$) (Tables 2, 3). While solid-state reduction could possibly cause this variation in mineral compositions, as discussed below, we suggest that the differences in mineralogy are more likely mostly due to compositional heterogeneities in the precursor chondritic material.

5.2. Heating and Partial Melting

Textural features and mineral compositions place constraints on the peak temperatures experienced by these rocks. Granoblastic textures, abundant triple junctions, and the presence of what appear to be recrystallized relict chondrules indicate that these rocks experienced peak temperatures at least comparable to those of type 6 chondrites (~750–950°C; Dodd, 1981). Although absolute temperature estimates from two-pyroxene geothermometry have considerable uncertainties, the values obtained for winonaites are 730–1200°C (Table 2). As these values represent minimum estimates of peak temperatures, it seems likely that winonaites were heated to higher peak temperatures than type 6 chondrites. In fact, peak temperatures likely exceed those needed to cause melting of the Fe,Ni-FeS assemblage at the cotectic temperature of ~950–980°C (Kullerud, 1963; Kubaschewski, 1982). The Fe,Ni-FeS cotectic melt is the first partial melt in a chondritic system and consists of ~85 wt% FeS and ~15 wt% Fe,Ni metal. We suggest that the metal and troilite veins found in Pontlyfni, QUE 94535, Winona and, possibly, Tierra Blanca are indicative of migration of Fe,Ni-FeS cotectic melts and are evidence for partial melting. Variability in the abundance of Fe,Ni-FeS veins in winonaites may reflect slight differences in the peak temperatures experienced by each meteorite or, alternatively, may simply reflect the somewhat random nature of melt migration in these rocks.

Silicates in a chondritic system begin to partially melt at temperatures around 1050°C, with the first melt being basaltic (plagioclase-pyroxene) in composition and plagioclase-rich (>55% plagioclase; Morse, 1980; Tuttle and Bowen, 1958). We suggest that the plagioclase-calcic pyroxene-rich areas in Pontlyfni are evidence for silicate partial melting, because the association of plagioclase and calcic pyroxene is typical of that expected from crystallization of a basaltic partial melt. The irregular, blobby outlines rather than vein-like shapes of these areas are suggestive of local melting without significant melt migration, although the irregular border with the surrounding matrix suggests local intrusion from the melt pocket into the matrix. Further evidence for silicate partial melting comes from the coarse-grained, olivine-rich areas found in Winona and Mount Morris (Wisconsin), which we interpret to be partial melt residues from elsewhere on the winonaite parent body that were incorporated into these rocks by impact mixing. The absence of coarse-grained pyroxene suggests that these areas did not form by local coarsening of the rock matrix. Taylor et al. (1993) calculated that olivine will be the only phase remaining in the residue of an H-chondrite precursor after 45% partial melting and, thus, the winonaite parent body where the coarse-grained, olivine-rich material formed must have experienced rather extensive silicate partial melting. Finally, although there is some uncertainty due to sampling considerations, the fractionated REE patterns of several winonaites are not inconsistent with silicate partial melting. The variable REE patterns may indicate local migration of REE-rich melts, probably formed by melting of plagioclase and phosphates, producing both REE-enriched and REE-depleted samples, sometimes within a single winonaite (e.g., Winona, Y-74025).

5.3. Impact Brecciation and Mixing of Lithologies

There is evidence that some winonaites experienced impact brecciation and mixing of lithologies. One line of evidence comes from the coarse-grained olivine-rich clumps described above, which we suggest could not have formed in situ in the rocks in which they are found. Rather, we suggest that they represent residual material of chondritic parentage that experienced at least 45% partial melting elsewhere on the winonaite parent body, and that this material was introduced into the rocks during impact brecciation and mixing. Further evidence of brecciation is found in Y-75300. This meteorite exhibits areas with two distinctly different grain sizes. We suggest that these lithologies represent material that experienced different peak temperatures elsewhere on the parent body and were mixed by impact processes. Since the various lithologies in winonaites experienced partial melting and some metamorphism (leading to differences in grain size) prior to mixing, brecciation must have occurred after peak temperatures had been reached.

5.4. Metamorphism and Cooling History

Metamorphism is responsible for the equigranular textures, abundant 120° triple junctions and the range of grain sizes found in winonaites (Fig. 2). This recrystallization and grain growth after impact mixing is responsible for obscuring the boundaries between different lithologies in Y-75300 and Winona. In agreement with King et al. (1981), we further suggest that the large poikilitic calcic pyroxene grains in Tierra Blanca formed by solid state metamorphism, rather than from a silicate melt. This suggestion is based on the observation that these pyroxenes are not associated with plagioclase, which would be expected if they had formed from a partial melt, and that growth of poikilitic pyroxene porphyroblasts by solid state metamorphism is well-known from terrestrial metamorphic rocks (e.g., de Wit and Strong, 1975; Kretz, 1994).

It seems clear that reduction also occurred to some extent during metamorphism and cooling. The winonaites generally have lower Fa in olivine than Fs in low-Ca pyroxene. This is indicative of solid-state reduction during cooling and consistent with the lower diffusion rates in low-Ca pyroxene relative to olivine (Huebner and Nord, 1981). In addition, Tierra Blanca

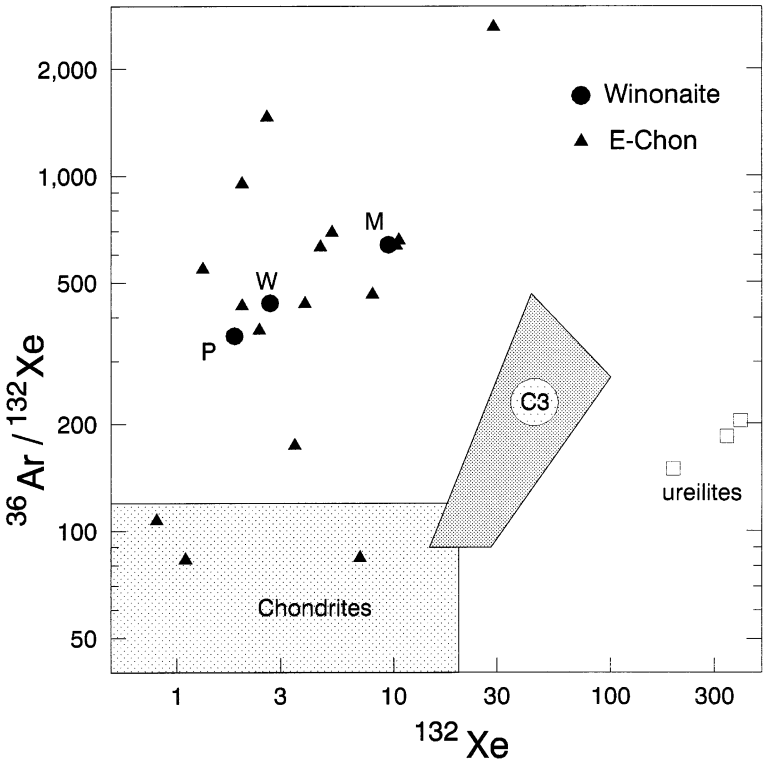

Fig. 10. Trapped ^{132}Xe concentrations (10^{-10} cm^{3}STP/g) and ^{36}Ar/^{132}Xe ratios for Mount Morris (Wisconsin), Winona and Pontlyfni, compared to those for ureilites and enstatite, ordinary and C3 chondrites (adopted from Crabb and Anders, 1981).

olivine and low-Ca pyroxene grains enclosed in the poikilitic calcic pyroxenes are significantly more FeO-rich than those in the matrix. This is consistent with the calcic pyroxene acting as a barrier to diffusion. Thus, the matrix mafic silicates experienced significantly greater levels of reduction during metamorphism. This also implies that solid-state growth of calcic pyroxenes predated reduction. Despite these indications of reduction in individual winonaites, it seems unlikely that the full range of mineral compositions and mineralogy observed in winonaites can be attributed solely to variable levels of reduction of a common precursor. One indication of this is the distribution of winonaite mineral compositions on a plot of Fa in olivine vs. Fs in low-Ca pyroxene (Fig. 8). If reduction from a common precursor occurred, we would expect a curved trend like that shown by the hatched line in Fig. 8, since diffusive reduction of FeO occurs more rapidly in olivine than low-Ca pyroxene. Instead, we observe a nearly linear trend. In addition, low-FeO winonaites contain reduced sulfide minerals (e.g., daubreélite), and it seems unlikely that these could have formed from oxidized minerals (e.g., chromite) during solid-state reduction. Thus, we attribute the overall variability in mineral compositions and mineralogy of winonaites to heterogeneities in the precursor chondritic material.

5.5. Trapped Noble Gases

Figure 10 compares the trapped ^{132}Xe concentrations and the trapped ^{36}Ar/^{132}Xe ratio in winonaites with the values typically found in ordinary and C3 chondrites (shaded areas), ureilites, and enstatite chondrites. Most ordinary chondrites show ^{36}Ar/^{132}Xe ratios of ~40–120, whereas many carbonaceous chondrites have higher ratios. It has been argued that ordinary and carbonaceous chondrites with ratios above ~120 contain solar-derived gases, in addition to a fractionated planetary component (Mazor et al., 1970; Crabb and Anders, 1981). Although ureilites contain the largest concentrations of trapped noble gases, their ^{36}Ar/^{132}Xe ratios are only slightly higher than those of most ordinary chondrites. In contrast, enstatite chondrites have trapped Xe concentrations similar to those of ordinary chondrites, but usually show ^{36}Ar/^{132}Xe ratios higher by several factors. These and other characteristics led Crabb and Anders (1981, 1982) to conclude that enstatite chondrites contain a solar-derived component of noble gases. This component was called "subsolar" to indicate that its Ar/Xe and Kr/Xe ratios are intermediate between planetary and solar compositions. The subsolar component is currently located in the enstatite phase, but may have been transferred to enstatite during metamorphism.

The ^{36}Ar/^{132}Xe ratios for the three winonaites are ~360–650, and they plot in Fig. 10 among the enstatite chondrite data. As is the case for enstatite meteorites, the ^{36}Ar/^{132}Xe ratio for winonaites tends to increase with increasing ^{132}Xe content, consistent with a mixture of planetary and "subsolar" components. The ^{84}Kr/^{132}Xe ratios for the three winonaites are 1.27–1.71 (considering only the melt extractions), but this ratio is not particularly diagnostic of the type of trapped gas. Trapped ^{84}Kr/^{132}Xe is ~1.0–1.5 for most ordinary and carbonaceous

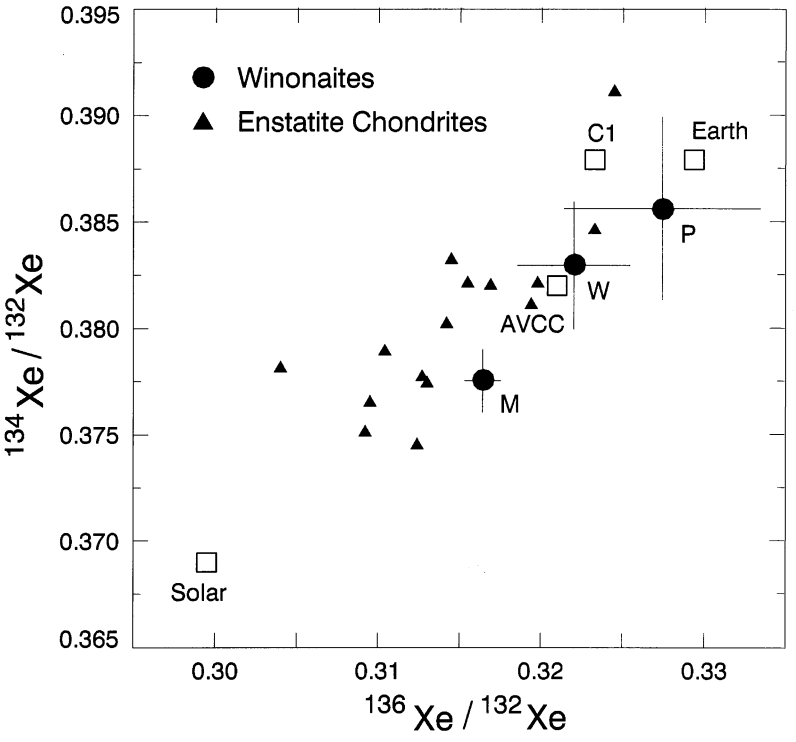

Fig. 11. Comparison of $^{134}Xe/^{132}Xe$ and $^{136}Xe/^{132}Xe$ isotopic ratios for Mount Morris (Wisconsin), Winona and Pontlyfni with those for enstatite chondrites (Crabb and Anders, 1981), the earth, the sun, and average carbonaceous chondrites (AVCC). C1 is a planetary composition derived by Pepin (1991).

chondrites and ureilites (Mazor et al., 1970) and ~2 for some silicate inclusions in iron meteorites (Bogard et al., 1971). Some analyses of enstatite chondrites give a $^{84}Kr/^{132}Xe$ ratio at least as high as ~4, but most enstatite chondrites show a ratio of ~2 for the case where the $^{36}Ar/^{132}Xe$ ratio is ~500 (Crabb and Anders, 1981). The mineral siting for trapped noble gases in winonaites is unknown, but is probably a silicate phase as it is for enstatites. Winonaites contain only trace amounts of carbon phases, which in primitive chondrites and ureilites occur in much larger abundances and are the carrier for much of the trapped noble gases.

The isotopic composition of Xe in winonaites also gives evidence for a solar-derived trapped component. Figure 11 compares the $^{134}Xe/^{132}Xe$ and $^{136}Xe/^{132}Xe$ ratios for Mount Morris (Wisconsin), Winona, and Pontlyfni with these values for the sun, Earth, carbonaceous and enstatite chondrites. Mount Morris (Wisconsin), which contains the largest amount of trapped Xe among these three winonaites, plots well toward the solar composition. Winona plots close to the composition of average carbonaceous chondrites (AVCC), but is displaced toward the solar composition compared to the hypothetical planetary composition C1 derived by Pepin (1991). Pontlyfni, which contains the least amount of trapped Xe and the largest analytical uncertainty, plots between the terrestrial and planetary compositions. Several enstatite chondrites containing "subsolar" Xe also plot between the solar and planetary compositions (Crabb and Anders, 1981). In addition to trapped Xe, all three winonaites also contain an obvious component of ^{129}Xe produced from the decay of extinct ^{129}I (Table 5).

5.6. Comparison of Ages of Winonaites and Silicate Inclusions in IAB irons

Similarities in mineralogy and oxygen isotopic compositions of winonaites and silicate inclusions in IAB irons suggest that both meteorite types may come from a common parent body (e.g., Benedix et al., 1998). It is therefore informative to compare ^{39}Ar-^{40}Ar ages of the three winonaites we dated with ^{39}Ar-^{40}Ar ages (Niemeyer, 1979) and K-^{40}Ar ages (Bogard et al., 1968) reported for silicate inclusions from several IAB iron meteorites. The ^{39}Ar-^{40}Ar ages for IABs must be reduced by a factor of 0.988, however, to correct for a subsequent change in age of the Saint Séverin flux/age monitor originally used (Herpfer et al., 1994). Silicates from Woodbine, Mundrabilla, Copiapo, and Pitts all gave relatively flat ^{39}Ar-^{40}Ar age profiles which yielded ages of 4.516 ± 0.030, 4.516 ± 0.030, 4.447 ± 0.030, and 4.487 ± 0.040 Ga, respectively. Classical K-^{40}Ar ages for Toluca and Four Corners are 4.507 ± 0.030 and 4.493 ± 0.030 Ga, respectively. The release profile for Landes shows considerably higher ages in the first ~40% of the ^{39}Ar release, but no indication at higher releases of implanted recoil ^{39}Ar. The second half of the ^{39}Ar release from Landes defines an age of 4.48 ± 0.03 Ga. None of the ^{39}Ar-^{40}Ar profiles for IAB silicates show post-formational loss of ^{40}Ar, except for modest loss suggested by Copiapo. Thus, the total range in K-Ar ages of IAB silicates is 4.447–4.516 Ga, with an average of 4.49 Ga.

The ^{39}Ar-^{40}Ar ages derived above for Pontlyfni (4.530–4.535 Ga), Winona (~4.51 Ga), and Mount Morris (Wisconsin) (≥4.40 Ga), give a broader range than those for silicate inclu-

sions in IABs. The well-defined age for Pontlyfni is distinctly older, which may suggest that IAB silicates remained open to diffusive loss of ^{40}Ar for a longer period. This could be consistent with IAB irons cooling at depth in their parent body, whereas winonaites were formed nearer to the surface and cooled more quickly. This suggestion is consistent with the faster metallographic cooling rate found for Winona (200°C/Myr; Kothari et al., 1981) compared to IAB irons (10–50°C/Myr; Herpfer et al., 1994). The lower limit for the age of Mount Morris (Wisconsin) is considerably less than the lowest IAB age and may represent heating due to impact.

6. SUMMARY

The winonaites are primitive achondrites that experienced limited partial melting and show evidence for brecciation and metamorphism on the precursor body. The precursor body was likely chondritic, but unlike any known chondrite group. Heating and partial melting, mixing, and metamorphism and cooling altered the precursor. Peak temperatures of up to 1200°C may have been reached prior to brecciation, but metamorphism and reduction also occurred after brecciation. ^{39}Ar-^{40}Ar age determinations and measurements of cosmogenic and trapped noble gases for Pontlyfni, Winona, and Mount Morris (Wisconsin) are consistent with the parent body history outlined here and indicate that these processes occurred early in the history of the solar system.

Acknowledgments—Samples of winonaites were kindly provided by R. S. Clarke, Jr. and G. J. MacPherson (Smithsonian Institution), M. M. Grady (British Museum), E. A. King (Univ. of Houston), A. J. Ehlmann (Texas Christian Univ.), the National Institute of Polar Research, and the Meteorite Working Group. Unpublished data on winonaite oxygen isotopic compositions were generously provided by R. N. Clayton. Helpful discussions were provided by G. J. Taylor, E. R. D. Scott, A. Meibom, and J. T. Wasson. Expert technical assistance was provided by T. Servilla and T. Hulsebosch. We wish to thank Tim Swindle, Monica Grady, and Andreas Weigel for helpful reviews. This study was funded in part by NASA grants NAGW-3281, NAG 5-4212, and NGT-51652 (K.Keil) and RTOP 152-14 (D. Bogard). This is Hawaii Institute of Geophysics and Planetology publication no. 1008 and School of Ocean and Earth Science and Technology publication no. 4665.

REFERENCES

Benedix G. K., McCoy T. J., Keil K., and Love S. G. (1998) A petrologic study of the IAB iron meteorites: Constraints on the formation of the IAB-winonaite parent body. *Meteoritics Planet Sci.* (submitted).

Bild R. W. (1977) Silicate inclusions in group IAB irons and a relation to the anomalous stones Winona and Mt. Morris (Wis.). *Geochim. Cosmochim. Acta* **41,** 1439–1456.

Bogard D., Burnett D., Eberhardt P., and Wasserburg G. J. (1968) ^{40}Ar-^{40}K ages of silicate inclusions in iron meteorites. *Earth Planet. Sci. Lett.* **3,** 275–283.

Bogard D. D., Huneke J. C., Burnett D. S., and Wasserburg G. J. (1971) Xenon and krypton analyses of silicate inclusions from iron meteorites. *Geochim. Cosmochim. Acta* **35,** 1231–1254.

Buchwald V. F. (1975) *Handbook of Iron Meteorites*. Univ. California Press.

Bunch T. E., Keil K., and Olsen E. (1970) Mineralogy and petrology of silicate inclusions in iron meteorites. *Contrib. Mineral. Petrol*. **25,** 297–340.

Choi B.-G., Ouyang X., and Wasson J. T. (1995) Classification and origin of IAB and IIICD iron meteorites. *Geochim. Cosmochim. Acta* **59,** 593–612.

Clayton R. N. and Mayeda T. K. (1988) Formation of ureilites by nebular processes. *Geochim. Cosmochim. Acta* **52,** 1313–1318.

Clayton R. N. and Mayeda T. K. (1996) Oxygen isotope studies of achondrites. *Geochim. Cosmochim. Acta* **60,** 1999–2017.

Crabb J. and Anders E. (1981) Noble gases in E-chondrites. *Geochim. Cosmochim. Acta* **45,** 2443–2464.

Crabb J. and Anders E. (1982) On the siting of noble gases in E-chondrites. *Geochim. Cosmochim. Acta* **46,** 2351–2361.

Davis A. M., Ganapathy R., and Grossman L. (1977) Pontlyfni: A differentiated meteorite related to the group IAB irons. *Earth Planet. Sci. Lett*. **35,** 19–24.

de Wit M. J. and Strong D. F. (1975) Eclogite-bearing amphibolites from the Appalachian mobile belt, northwestern Newfoundland; dry versus wet metamorphism. *J. Geol.* **83,** 609–627.

Dodd R. T. (1981) *Meteorites: A Chemical-Petrologic Synthesis*. Cambridge Univ. Press.

Eugster O. (1988) Cosmic ray production rates for ^{3}He, ^{21}Ne, ^{38}Ar, ^{83}Kr, and ^{126}Xe in chondrites based on ^{81}Kr-Kr exposure ages. *Geochim. Cosmochim. Acta* **52,** 1649–1662.

Eugster O., Michel Th., Niedermann S., Wang D., and Yi W. (1993) The record of cosmogenic, radiogenic, fissiogenic, and trapped noble gases in recently recovered Chinese and other chondrites. *Geochim. Cosmochim. Acta* **57,** 1115–1142.

Gaffey M. J., Burbine T. H., and Binzel R. P. (1993) Asteroid spectroscopy: Progress and perspectives. *Meteoritics* **28,** 161–187.

Gomes C. B. and Keil K. (1980) *Brazilian Stone Meteorites*. Univ. New Mexico Press.

Gooding J. L. and Keil K. (1981) Relative abundances of chondrule primary textural types in ordinary chondrites and their bearing on conditions of chondrule formation. *Meteoritics* **16,** 17–43.

Graham A. L., Easton A. J., and Hutchison R. (1977) Forsterite chondrites—the meteorites Kakangari, Mount Morris (Wisconsin), Pontlyfni, and Winona. *Mineral. Mag.* **41,** 201–210.

Herpfer M. A., Larimer J. W., and Goldstein J. I. (1994) A comparison of metallographic cooling rate methods used in meteorites. *Geochim. Cosmochim. Acta* **58,** 1353–1366.

Huebner J. S. and Nord G. L., Jr. (1981) Assessment of diffusion in pyroxene: What we do and do not know (abstr.). *Lunar Planet. Sci.* **12,** 479–481.

Huneke J. C. and Smith S. P. (1976) The realities of recoil out of small grains and anomalous age patterns in ^{39}Ar-^{40}Ar dating. *Proc. Lunar Sci. Conf.* **7,** 1987–2008.

Kallemeyn G. W. (1996) Pontlyfni: Not just another winonaite (abstr.). *Meteoritics and Planet. Sci.* **31,** A68–A69.

Kallemeyn G. W. and Wasson J. T. (1985) The compositional classification of chondrites: IV. Ungrouped chondritic meteorites and clasts. *Geochim. Cosmochim. Acta* **49,** 261–270.

Keil K. (1968) Mineralogical and chemical relationships among enstatite chondrites. *J. Geophys. Res.* **73,** 6945–6976.

Kennedy B. M. (1981) Potassium-argon and iodine-xenon gas retention ages of enstatite chondrite meteorites. Ph.D. Dissertation, Washington Univ.

Kimura M., Tsuchiyama A., Fukuoka T., and Iimura Y. (1992) Antarctic primitive achondrites, Yamato-74025, -75300, and -75305: Their mineralogy, thermal history, and the relevance to winonaite. *Proc. NIPR Symp. Antarct. Meteorites* **5,** 165–190.

King E. A., Jarosewich E., and Daugherty F. W. (1981) Tierra Blanca: An unusual achondrite from West Texas. *Meteoritics* **16,** 229–237.

Kothari B. K., Maggiore P., and Scott E. R. D. (1981) Winona meteorite: Fission track ages and thermal history. *Carnegie Inst. Wash. Yearbook* **80,** 527–530.

Kretz R. (1982) Transfer and exchange equilibria in a portion of the pyroxene quadrilateral as deduced from natural and experimental data. *Geochim. Cosmochim. Acta* **46,** 411–421.

Kretz R. (1994) *Metamorphic Crystallization*. John Wiley & Sons.

Kubaschewski O. (1982) *Iron-Binary Phase Diagram.* Springer.

Kullerud G. (1963) The Fe-Ni-S system. *Ann. Rep. Geophys. Lab*. **67,** 4055–4061.

Lindsley D. H. and Andersen D. J. (1983) A two-pyroxene thermometer. *Proc. Lunar Planet. Sci. Conf.* **13,** A887–A906.

Lusby D., Scott E. R. D, and Keil K. (1987) Ubiquitous High-FeO Silicates in Enstatite Chondrites *Proc. 17th Lunar Planet. Sci. Conf. Part 2, J. Geophys. Res.* **92,** E679–E695.

Mason B. (1996) Thin section description of QUE 94535. *Antarctic Meteor. Newslett.* **19,** No. 1, 18.
Mason B. and Jarosewich E. (1967) The Winona meteorite. *Geochim. Cosmochim. Acta* **31,** 1097–1099.
Mazor E., Heymann D., and Anders E. (1970) Noble gases in carbonaceous chondrites. *Geochim. Cosmochim. Acta* **34,** 781–824
McCoy T. J., Scott E. R. D., and Haack H. (1993) Genesis of the IIICD iron meteorites: Evidence from silicate-bearing inclusions. *Meteoritics* **28,** 552–560.
McCoy T. J. et al. (1996) A petrologic, chemical and isotopic study of Monument Draw and comparison with other acapulcoites: Evidence for formation by incipient partial melting. *Geochim. Cosmochim. Acta* **60,** 2681–2708.
McCoy T. J. et al. (1997a) A petrologic and isotopic study of lodranites: Evidence for early formation as partial melt residues from heterogeneous precursors. *Geochim. Cosmochim. Acta* **61,** 623–638.
McCoy T. J., Keil K., Muenow D. W., and Wilson L. (1997b) Partial melting and melt migration on the acapulcoite-lodranite parent body. *Geochim. Cosmochim. Acta* **61,** 639–650.
McSween H.Y. Jr., Bennett M. E., III, and Jarosewich E. (1991) The mineralogy of ordinary chondrites and implications for asteroid spectrophotometry. *Icarus* **90,** 107–116.
Mittlefehldt D. W., Lindstrom M. M., Bogard D. D., Garrison D. H., and Field S. W. (1996) Acapulco- and Lodran-like achondrites: Petrology, geochemistry, chronology and origin. *Geochim. Cosmochim. Acta* **60,** 867–882.
Morse S. A. (1980) *Basalts and Phase Diagrams*. Springer-Verlag.
Nagahara H. (1992) Yamato-8002: Partial melting residue on the "unique" chondrite parent body. *Proc. NIPR Symp Antarctic Meteorites* **5,** 191–223.
Nehru C. E., Prinz M., Weisberg M. K., Ebihara M. E., Clayton R. N., and Mayeda T. K. (1996) A new brachinite and petrogenesis of the group. *Lunar Planet. Sci.* **27,** 943–944 (abstr.).
Niemeyer S. (1979) ^{40}Ar-^{39}Ar dating of inclusions from IAB iron meteorites. *Geochim. Cosmochim. Acta* **43,** 1829–1840.
Pepin R. O. (1991) On the origin and early evolution of terrestrial planet atmospheres and meteoritic volatiles. *Icarus* **92,** 2–79.
Prinz M., Waggoner D. G., and Hamilton P. J. (1980) Winonaites: A primitive achondritic group related to silicate inclusions in IAB irons. *Lunar Planet. Sci.* **11,** 902–904 (abstr.).
Prinz M., Nehru C. E., Delaney J. S., and Weisberg M. (1983) Silicates in IAB and IIICD irons, winonaites, lodranites and Brachina: A primitive and modified primitive group. *Lunar Planet. Sci.* **14,** 616–617 (abstr.).
Schultz L. et al. (1982) Allan Hills A77081—An unusual stony meteorite. *Earth Planet. Sci. Lett.* **61,** 23–31.
Stöffler D., Keil K., and Scott E. R. D. (1991) Shock metamorphism of ordinary chondrites. *Geochim. Cosmochim. Acta* **55,** 3845–3867.
Swindle T. D., Kring D. A., Burkland M. K., Hill D. H., and Boynton W. V. (1998) Noble gases, bulk chemistry, and petrography of olivine-rich achondrites Eagles Nest and LEW 88763: Comparison to brachinites. *Meteoritics Planet. Sci.* **33,** 31–48.
Takeda H., Mori H., Hiroi T., and Saito J. (1994) Mineralogy of new Antarctic achondrites with affinity to Lodran and a model of their evolution in an asteroid. *Meteoritics* **29,** 830–842.
Taylor G. J., Keil K., McCoy T., Haack H., and Scott E. R. D. (1993) Asteroid differentiation: Pyroclastic volcanism to magma oceans. *Meteoritics* **28,** 34–52.
Turner G., Enright M. C., and Cadogan P. H. (1978) The early history of chondrite parent bodies inferred from ^{39}Ar-^{40}Ar ages. *Proc. Lunar Planet. Sci. Conf.* **9,** 989–1025.
Tuttle O. F. and Bowen N. L. (1958) *Origin of granite in the light of experimental studies in the system* $NaAlSi_3O_8$-$KAlSi_3O_8$-SiO_2-H_2O. Memoir 74, Geol. Soc. America.
Van Schmus W. R. and Ribbe P. H. (1968) The composition and structural state of feldspar from chondritic meteorites. *Geochim. Cosmochim. Acta* **32,** 1327–1342.
Weisberg M. K., Boesenberg J. S., Kozhushko G., Prinz M., Clayton R. N., and Mayeda T. K. (1995) EH3 and EL3 chondrites: A petrologic-oxygen isotopic study. *Lunar Planet. Sci.* **26,** 1481–1482 (abstr.).
Yamamoto K., Nakamura N., Misawa K., Yanai K., and Matsumoto Y. (1991) Lithophile trace element abundances in Antarctic unique meteorites and in unique clasts from L6 chondrites (abstr.). *Papers 15th Symp. Antarctic Met.*, 97–98. NIPR.
Yanai K. and Kojima H. (1995) *Catalog of the Antarctic Meteorites*. NIPR.
Yugami K., Takeda H., Kojima H., and Miyamoto M. (1996) Mineralogy of new primitive achondrites, Y8005 and Y8307 and their differentiation from chondritic materials. *Papers 21st Symp. Antarctic Met.*, 216–218 (abstr.).
Zähringer J. (1968) Rare gases in stony meteorites. *Geochim. Cosmochim. Acta* **32,** 209–237.

Appendix Winonaite Ar age data. Columns are, from left to right: extraction temperature, concentration of ^{39}Ar, calculated age in Ga, the K/Ca elemental ratio, and the $^{40}Ar/^{39}Ar$, $^{38}Ar/^{39}Ar$, $^{37}Ar/^{39}Ar$, and $^{36}Ar/^{39}Ar$ ratios, respectively. Uncertainties are shown beneath all ratios and the ages. The ^{39}Ar concentrations and K/Ca, $^{38}Ar/^{39}Ar$, and $^{36}Ar/^{39}Ar$ ratios have been multiplied by the factors indicated. The weight of each sample analyzed is given as well as the irradiation constant (J value) used in calculating ages.

Temp. °C	^{39}Ar cc/g x10^{9}	AGE ± Ga	K/Ca ± x100	40/39 ±	38/39 ± x100	37/39 ±	36/39 ± x100
Pontlyfni (0.0233g, J=0.05860)							
400	1.55	4.359	18.96	174.1	200.6	2.90	304.29
		0.065	14.93	6.9	21.2	2.28	36.22
500	0.91	4.052	43.36	144.2	48.6	1.27	31.88
		0.037	16.33	3.3	2.6	0.48	2.15
600	2.49	4.640	113.06	206.4	12.01	0.49	10.10
		0.019	13.18	2.2	0.46	0.06	0.65
675	7.98	4.671	21.00	210.2	5.93	2.62	4.57
		0.008	0.22	0.7	0.21	0.03	0.38
725	19.04	4.588	49.37	200.0	4.02	1.11	2.72
		0.006	0.50	0.3	0.15	0.01	0.13
750	13.74	4.538	40.52	194.0	4.43	1.36	3.33
		0.007	0.42	0.4	0.16	0.01	0.16
775	12.40	4.531	48.72	193.2	4.46	1.13	2.92
		0.007	0.50	0.5	0.16	0.01	0.16
800	15.68	4.532	52.65	193.4	4.44	1.04	2.73
		0.006	0.54	0.4	0.15	0.01	0.12
825	26.69	4.542	67.72	194.5	5.01	0.81	3.12
		0.006	0.68	0.3	0.13	0.01	0.23
850	18.53	4.531	58.90	193.2	5.66	0.93	3.77
		0.007	0.60	0.4	0.15	0.01	0.11
875	8.67	4.533	51.32	193.5	6.37	1.07	4.42
		0.008	0.54	0.7	0.20	0.01	0.22
925	17.83	4.532	19.50	193.4	20.62	2.82	15.98
		0.006	0.20	0.4	0.16	0.03	0.13
1000	9.19	4.521	16.01	192.1	40.75	3.44	30.69
		0.008	0.17	0.7	0.29	0.04	0.31
1100	37.86	4.522	14.17	192.2	10.08	3.88	16.37
		0.006	0.14	0.3	0.14	0.04	0.08
1200	66.14	4.524	9.45	192.4	11.5	5.82	22.15
		0.006	0.09	0.2	0.13	0.06	0.29
1250	15.80	4.531	1.90	193.2	35.54	28.90	68.75
		0.007	0.02	0.4	0.18	0.30	0.23
1350	10.60	4.539	1.29	194.2	79.41	42.78	227.25
		0.010	0.01	0.9	0.54	0.47	1.45
1550	3.98	4.532	1.98	193.3	140.1	27.72	533.71
		0.035	0.05	4.1	4.1	0.65	15.54
Winona (0.03022g, J=0.06006)							
350	6.08	6.030	6.99	454.2	334.8	7.87	169.25
		0.007	0.07	1.3	10.	0.08	0.58
400	1.15	2.890	11.45	66.0	140.7	4.80	82.17
		0.040	0.34	1.8	5.3	0.14	3.25
500	2.00	3.549	12.76	102.4	103.9	4.31	42.04
		0.026	0.25	1.7	2.4	0.08	1.26
600	3.16	4.045	16.22	140.1	52.46	3.39	19.32
		0.015	0.21	1.2	0.70	0.04	0.58
675	10.38	4.396	26.55	173.8	16.32	2.07	13.07
		0.007	0.48	0.5	0.18	0.04	0.17

Appendix.Continued

725	15.05	4.366	45.46	170.6	7.80	1.21	7.48
		0.006	0.46	0.3	0.15	0.01	0.11
775	30.32	4.355	38.69	169.4	7.35	1.42	4.39
		0.006	0.39	0.2	0.13	0.01	0.06
800	23.11	4.369	32.75	170.9	8.34	1.68	3.73
		0.006	0.33	0.2	0.14	0.02	0.07
825	29.46	4.384	27.44	172.4	12.21	2.00	5.37
		0.006	0.28	0.2	0.13	0.02	0.06
850	34.93	4.410	14.20	175.2	18.94	3.87	8.99
		0.006	0.14	0.2	0.14	0.04	0.21
875	33.01	4.438	19.90	178.3	26.40	2.76	10.84
		0.006	0.20	0.2	0.14	0.03	0.06
900	26.45	4.455	19.19	180.0	33.32	2.87	13.31
		0.006	0.19	0.2	0.15	0.03	0.07
950	37.33	4.456	14.13	180.2	52.95	3.89	21.21
		0.006	0.14	0.2	0.15	0.04	0.05
1000	25.17	4.461	10.30	180.7	85.50	5.34	31.13
		0.006	0.10	0.2	0.22	0.05	0.10
1100	70.71	4.430	5.10	177.4	104.1	10.79	34.49
		0.006	0.05	0.1	0.2	0.11	0.06
1150	12.60	4.513	1.12	186.5	216.9	48.92	205.7
		0.006	0.01	0.4	0.5	0.50	0.5
1250	6.05	4.506	0.33	185.7	728.3	166.26	845.6
		0.013	0.00	1.4	6.2	2.07	7.4
1350	3.53	4.432	0.54	177.6	1547.6	101.86	1362.1
		0.021	0.01	2.2	25.8	1.63	22.7
1550	0.72	4.616	1.93	198.5	893.2	28.43	726.9
		0.066	0.08	7.9	49.0	1.16	40.0
Mt. Morris (0.02747g, J=0.05476)							
400	20.21	3.342	45.55	98.2	136.0	1.21	51.96
		0.006	0.46	0.2	0.3	0.01	0.12
500	2.87	1.950	26.51	35.6	75.96	2.07	67.60
		0.026	0.63	0.8	2.33	0.05	2.07
600	2.32	2.726	70.81	64.5	52.68	0.78	59.81
		0.033	1.80	1.5	1.80	0.02	2.09
725	10.89	3.919	34.44	142.0	21.81	1.60	32.41
		0.008	0.36	0.4	0.19	0.02	0.22
750	5.90	4.310	18.00	180.9	9.50	3.06	16.16
		0.009	0.20	0.8	0.24	0.03	0.32
775	54.55	4.309	11.75	180.7	13.27	4.68	28.99
		0.006	0.12	0.2	0.14	0.05	0.05
800	0.81	3.514	2.23	109.8	27.55	24.64	52.32
		0.087	0.13	6.2	2.27	1.40	4.13
850	1.39	4.114	3.16	160.3	19.13	17.40	54.23
		0.032	0.07	3.2	0.92	0.38	1.99
900	2.08	4.399	9.37	190.9	21.75	5.87	83.22
		0.021	0.15	2.3	0.65	0.09	1.52
950	3.14	4.381	6.50	188.9	26.74	8.47	100.12
		0.015	0.08	1.6	0.48	0.11	1.22
1000	4.82	4.384	4.44	189.2	34.47	12.40	118.01
		0.011	0.05	1.0	0.36	0.14	0.90
1050	6.28	4.425	2.50	193.9	50.98	21.98	163.32
		0.009	0.03	0.9	0.37	0.24	0.93
1100	4.67	4.403	0.95	191.4	133.8	57.76	441.26
		0.012	0.01	1.2	1.0	0.68	3.29
1150	1.24	4.128	0.14	161.8	1267	388.7	5222.9
		0.052	0.00	5.1	48	12.9	196.9
1250	0.72	3.843	0.08	135.5	6343	682.2	29614
		0.116	0.01	9.9	347	50.3	2555
1350	0.41	3.909	0.16	141.2	12376	353.1	60869
		0.102	0.01	9.0	547	22.8	4893
1550	0.28	3.404	0.44	102.3	4900	126.2	21816
		0.413	0.12	27.6	1789	34.0	7963